Phase transformations and compatibility in helical structures

Fan Feng, Paul Plucinsky, Richard D. James*

Department of Aerospace Engineering and Mechanics, University of Minnesota, United States

ARTICLE INFO

ABSTRACT

We systematically study phase transformations from one helical structure to another. Motivated in part by recent work that relates the presence of compatible interfaces with properties such as the hysteresis and reversibility of a phase transformation (Chluba et al., 2015; Ni et al., 2016; Zarnetta et al., 2010; Song et al., 2013), we give necessary and sufficient conditions on the structural parameters of two helical phases such that they are compatible. We show that, locally, four types of compatible interface are possible: vertical, horizontal, helical and elliptical. We discuss the mobility of these interfaces and give examples of systems of interfaces that are mobile and could be used to fully transform a helical structure from one phase to another.

These results provide a basis for the tuning of helical structural parameters so as to achieve compatibility of phases. In the case of transformations in crystals, this kind of tuning has led to materials with exceptionally low hysteresis and dramatically improved resistance to transformational fatigue. Compatible helical transformations with low hysteresis and fatigue resistance would exhibit an unusual shape memory effect involving both twist and extension, and may have potential applications as new artificial muscles and actuators.

© 2019 Elsevier Ltd. All rights reserved.

1. Introduction

A *helical structure* is a molecular structure obtained by taking the orbit of a single molecule under a *helical group*. The helical groups are the discrete groups of isometries (i.e., orthogonal transformations and translations) that do not contain any pure translations and do not fix a point. Helical structures are special cases of the more general concept of *objective structures* (James, 2006). An objective structure is a discrete collection of atoms where corresponding atoms in each molecule "see the same environment". For reasons that are not understood and are related to the celebrated and far-from-solved "crystallization problem", objective structures are surprisingly well-represented among scientifically and technologically important nanostructures.

Helical structures, in particular, are ubiquitous. Single-walled carbon nanotubes of any chirality as well as many biological molecules are helical. They are especially common in non-animal viruses. An example of a helical structure that undergoes a phase transformation of the type discussed here is the tail sheath of bacteriophage T4 (Moody, 1967; 1973). This highly effective transformation is employed by the T4 virus to drive the stiff tail tube through the cell wall of the host, and the viral DNA then enters the host through the tail tube. It can be seen that, aside from being helical, this transformation has many features in common with martensitic phase transformations in crystals as first noticed by Olson and Hartman (1982), such as being diffusionless, and exhibiting a large coordinated shape change. The transformation also exhibits a latent heat

---

* Corresponding author.
   E-mail addresses: fengx258@umn.edu (F. Feng), pplucins@umn.edu (P. Plucinsky), james@umn.edu (R.D. James).

(Arisaka et al., 1981), and the transformation can be accurately modeled by a free energy of the type used in studies of phase transformations in crystals (Falk and James, 2006). The forms of the helical generators of both phases of this tail tube are special cases of those studied here, but the phases of bacteriophage T4 do not precisely satisfy the strong conditions of compatibility found here. This is possibly related to the fitness requirement of T4 to have sufficiently large hysteresis so that the transformation does not occur spontaneously. In fact, T4 has a trigger involving its tail fibers and baseplate which induces the transformation only after it has attached itself to its host.

Another typical example is the phase transformation of bacterial flagella, which are mechanically induced by the bacterium's molecular motor (Asakura, 1970; Calladine, 1975; Yonekura et al., 2003). The bacterium can enter into "swimming" mode to move toward a favorable chemical and thermal environment, or a "tumbling" mode to alter its direction, by switching chirality of the flagellum. The thermodynamics of such phenomena was explained by minimizing Gibbs free energy, including chemical and mechanical parts, and thermomechanical phase diagrams are given in Komai (2015). Other examples analyzed in Section 8 are certain microtubules satisfying closely the compatibility conditions derived here. Some widely studied nonbiological helical structures are the celebrated carbon nanotubes (any chirality) and the nanotubes BCN (Zhou et al., 2014), GaN (Goldberger et al., 2003), MoS_2 and WS_2 (Radisavljevic et al., 2011; Zhang et al., 2010).

A recent development that can guide the tuning of lattice parameters is an implementation of density functional theory that incorporates helical symmetry, so that typical total energy calculations on nanotubes with no axial periodicity can be carried out with a few atom calculation[1] (Banerjee, 2013; Banerjee et al., 2015; Banerjee and Suryanarayana, 2016; 2018). With these tools many different twisted and extended nanotubes can be evaluated and phase transformations can be identified. Twist and extension are not only valuable parameters to seek novel phase transformations, but they can also be used to seek special conditions of compatibility identified here. Phase transformations having a change in magnetoelectric or transport properties (Banerjee and Suryanarayana, 2018) are particularly interesting in an engineering context due to the wire-like geometry of nanotubes, together with the fact that their lengths can be macroscopic.

In this paper we develop a theory of diffusionless phase transformations in helical structures with a focus on low energy interfaces. The main guideline behind this study is to systematically replace the translation group by the helical group, but to otherwise exploit the patterns of thought used in atomistic and continuum theories of phase transformations (Ball and James, 1987; 1992; Bhattacharya, 1992; James, 2015; James and Hane, 2000; Song et al., 2013). We show that familiar concepts from phase transformations in crystals such as *variants*, *twins*, *compatible interfaces*, *slip planes* and *habit planes* have analogs in the helical case, though the analogy is not perfect.

To develop a phase transformation theory for helical structures, we consider structures generated by the largest Abelian discrete helical group acting on a finite set of points in $\mathbb{R}^3$, as described in Section 2 (explicitly, Eq. (3)). This assumption includes structures generated by all the helical groups as long as we choose the generating molecule appropriately, as we explain below. We then focus on compatible interfaces. Compatibility is fundamentally a metric property, i.e., it concerns conditions under which atoms that are close together before transformation remain close together after transformation. However, closeness of powers of group generators does not generally imply closeness of molecules. Therefore, we are led to develop a reparameterization of the group by *nearest neighbor generators*, as well as a suitable domain—analogous to a reference configuration of continuum mechanics—of powers of the generators that imply a 1–1 relation between powers and molecules with convenient metric properties. The reparameterization of the groups in terms of nearest neighbor generators and the characterization of their domains is presented as a series of rigorously derived algorithms in Section 3.

The powers of the nearest neighbor generators are integers, and induce a formula for molecular positions from a suitable domain of the $\mathbb{Z}^2$ lattice to the helical structure. We notice that the formula makes sense for non-integer values of the powers and still the metric properties hold: closeness of powers (whether integer or not) implies closeness of molecules. Thus, this formula can be thought of as a *deformation* from an analogous reference domain of $\mathbb{R}^2$ to the helical structure. Using this observation, we then define compatibility in continuum mechanics terms (cf., Ganor et al. (2016)) in Section 4 via Eq. (17) for the induced deformations of the two helical phases. Further, we work out all local solutions for compatible interfaces for all values of the group parameters (under mild restrictions) in Section 5, and we give explicit closed form formulas for all compatible interfaces (Theorems 5.1 and 5.2). The conditions on group parameters for compatible interfaces that we find are strictly analogous to the condition $\lambda_2 = 1$ in theories of phase transformations in crystals (Cui et al., 2006; James and Zhang, 2005; Zarnetta et al., 2010; Zhang et al., 2009). We conjecture that the dramatic reduction of the sizes of hysteresis loops observed in transforming crystals when λ_2 is tuned to the value 1 by compositional changes will also occur in helical structures when the conditions found here are satisfied.

Some of the local interfaces we find can all be extended to form loops or infinite lines (Section 5.2). Moreover, one can combine various compatible interfaces to form nanostructures that are analogous to supercompatible interfaces in crystals (Chen et al., 2013; Gu et al., 2018). In particular in Section 8 we find an interesting helical analog of an austenite/martensite interface seen in supercompatible bulk crystals (Chen et al., 2013; Chluba et al., 2015; Ni et al., 2016; Song et al., 2013): it is moveable without slip and involves twinning, exhibits no stressed transition layer, but otherwise looks very different from usual austenite/martensite interfaces.

An important special case is that in which the two phases are the same, i.e., the two helical lattices are related by an orthogonal transformation and translation. In this case the compatible interfaces we find are naturally interpreted as helical

---

[1] two atoms for twisted/extended chiral C nanotubes.

analogs of slips or twins. We study this case in Sections 6 and 7. Again, some exact analogs with the crystalline case (e.g., mirror symmetry) emerge, but there are also cases that have no crystalline analog.

It should be noted that interfaces of the type identified here in atomic structures are also seen in macroscopic hollow tubes made of NiTi shape memory material (He and Sun, 2009). For related theory at macroscopic level see also (Ganor et al., 2016).

2. Isometry groups and helical structures

As noted in the introduction, a helical structure is the orbit of a molecule under a helical group. To define this precisely, let $\mathbf{p}_1, \ldots, \mathbf{p}_M$ be the average positions of atoms in a molecule (with corresponding species). A helical group can be represented schematically by $\{g_0, g_1, g_2, \ldots\}$ with say $g_0 = identity$. Consequently, a helical structure is given by $\{g_0(\mathbf{p}_1), \ldots, g_0(\mathbf{p}_M)\} \cup \{g_1(\mathbf{p}_1), \ldots, g_1(\mathbf{p}_M)\} \cup \{g_2(\mathbf{p}_1), \ldots, g_2(\mathbf{p}_M)\} \cup \ldots$.

A helical group is a discrete group consisting of *isometries* that do not fix a point and which does not contain any pure translations. That is, each g_i, $i = 0, 1, 2, \ldots$, is an isometry of the form $(\mathbf{Q}_i|\mathbf{c}_i)$ in conventional notation, where $\mathbf{Q}_i$ is an orthogonal transformation on $\mathbb{R}^3$ and $\mathbf{c}_i \in \mathbb{R}^3$. The condition that group contains no translation is $(\mathbf{Q}_i|\mathbf{c}_i) \neq (\mathbf{I}|\mathbf{c})$ for any $\mathbf{c} \neq 0$, and the condition that the group does not fix a point is that there is no $\mathbf{x}_0 \in \mathbb{R}^3$ such that $(\mathbf{Q}_i - \mathbf{I})\mathbf{x}_0 + \mathbf{c}_i = 0$ for every i. (If there is such an $\mathbf{x}_0$, the resulting group is a point group.) The group product is $g_i g_j = (\mathbf{Q}_i \mathbf{Q}_j | \mathbf{Q}_i \mathbf{c}_j + \mathbf{c}_i)$, the identity is $g_0 = (\mathbf{I}|0)$, and the inverses are $g_i^{-1} = (\mathbf{Q}_i^T | -\mathbf{Q}_i^T \mathbf{c}_i)$. Further, the action of g_i on $\mathbf{p} \in \mathbb{R}^3$, as indicated above, is simply $g_i(\mathbf{p}) = \mathbf{Q}_i \mathbf{p} + \mathbf{c}_i$. Finally, the *orbit* of $\mathbf{p}$ is the collection $g_0(\mathbf{p}), g_1(\mathbf{p}), g_2(\mathbf{p}), \ldots$

Volume E of the International Tables of Crystallography (IT) contains a listing of *subperiodic groups*, i.e., the discrete isometry groups not containing a full set of 3 linearly independent translations. By definition, helical groups are discrete isometry groups containing no translations, and so they would appear to fall under the umbrella of this classification. However, as is known to crystallographers, Volume E of IT does not contain the helical groups. This is due to an unfortunate feature of the scheme by which IT is organized. That is, in IT two isometry groups G_1 and G_2 are considered the same if they are related by an affine transformation, $G_2 = a G_1 a^{-1}$ where $a = (\mathbf{A}|\mathbf{c})$, $\det \mathbf{A} \neq 0$ (or, for some parts of IT, $\det \mathbf{A} > 0$). Here the product rule is the same as the one given above[2]. By this classification, there are infinitely many helical groups and a listing according to the scheme of IT is impossible. For example, by this classification scheme, the simple helical group specified in (1) below is actually an infinite number of different groups, one for each distinct choice of the angle[3] θ.

For the purpose of this paper, and, one could argue, for many other purposes in science and engineering, the affine equivalence is not relevant, as one would often like to know "what are all the groups". Indeed, for the purpose of exploring conditions of compatibility, we need explicit formulas for the groups with all the free parameters displayed[4] We have rigorously derived the formulas for all the helical groups in this way (Dayal et al., 2018). From this, every helical group is given by one of the four formulas (as illustrated in Fig. 1):

$$\{h^m : m \in \mathbb{Z}\}, \tag{1}$$

$$\{h^m f^s : m \in \mathbb{Z}, \, s = 1, 2\}, \tag{2}$$

$$\{h^m g^n : m \in \mathbb{Z}, \, n = 1, \ldots, i\}, \tag{3}$$

$$\{h^m g^n f^s : m \in \mathbb{Z}, \, n = 1, \ldots, i, \, s = 1, 2\}, \tag{4}$$

where

1. $h = (\mathbf{Q}_\theta | \tau \mathbf{e} + (\mathbf{I} - \mathbf{Q}_\theta)\mathbf{z})$, $\mathbf{Q}_\theta \mathbf{e} = \mathbf{e}$, $|\mathbf{e}| = 1$, $\mathbf{z} \in \mathbb{R}^3$, $\tau \in \mathbb{R} \setminus \{0\}$, is a screw displacement with an angle θ that is an irrational multiple of 2π.
2. $g = (\mathbf{Q}_\alpha | (\mathbf{I} - \mathbf{Q}_\alpha)\mathbf{z})$, $\mathbf{Q}_\alpha \mathbf{e} = \mathbf{e}$, is a proper rotation with angle $\alpha = 2\pi / i$, $i \in \mathbb{N}$, $i \neq 0$.
3. $f = (\mathbf{Q} | (\mathbf{I} - \mathbf{Q})\mathbf{z}_1)$, $\mathbf{Q} = -\mathbf{I} + 2\mathbf{e}_1 \otimes \mathbf{e}_1$, $|\mathbf{e}_1| = 1$, $\mathbf{e} \cdot \mathbf{e}_1 = 0$ is a 180° rotation with axis perpendicular to $\mathbf{e}$. Here, $\mathbf{z}_1 = \mathbf{z} + \xi \mathbf{e}$, for some $\xi \in \mathbb{R}$.

Groups (1) and (3) are Abelian (the elements commute) and clearly (1) is a subgroup of (3)[5]. Groups (2) and (4) are not Abelian because the element f does not commute with g or h. However, note that $f^2 = identity$. Thus, the action of f on a suitable molecule produces a nearby molecule. Then, to get the full structure in the orbit of (4), we operate the group (3) on this pair of molecules. If the structure is reasonably dense with molecules, we can always consider this pair to be close together, since there will be some molecule close to the axis through $\mathbf{e}_1$. (Note that $\mathbf{e}_1$ is perpendicular to the axis of the cylinder on which the structure lies.) But, if this pair is close together, then we can reasonably discuss compatibility in

---

[2] For $\mathbf{Q}_i^T$ substitute $\mathbf{A}^{-1}$.

[3] that is, there is no affine transformation which relates $\{h^m : m \in \mathbb{Z}\}$ and $\{\tilde{h}^m : m \in \mathbb{Z}\}$ for $\theta \neq \tilde{\theta}$. (see (1) for notation).

[4] Abstract groups (multiplication tables) are not so useful, and for the applications in this paper it does not matter if the abstract group suddenly gets bigger at a particular set of values of the parameters.

[5] Indeed, if we restrict our attention to the case $i = 1$ for the groups in (3), then $g = id$ and we obtain the groups in (1).
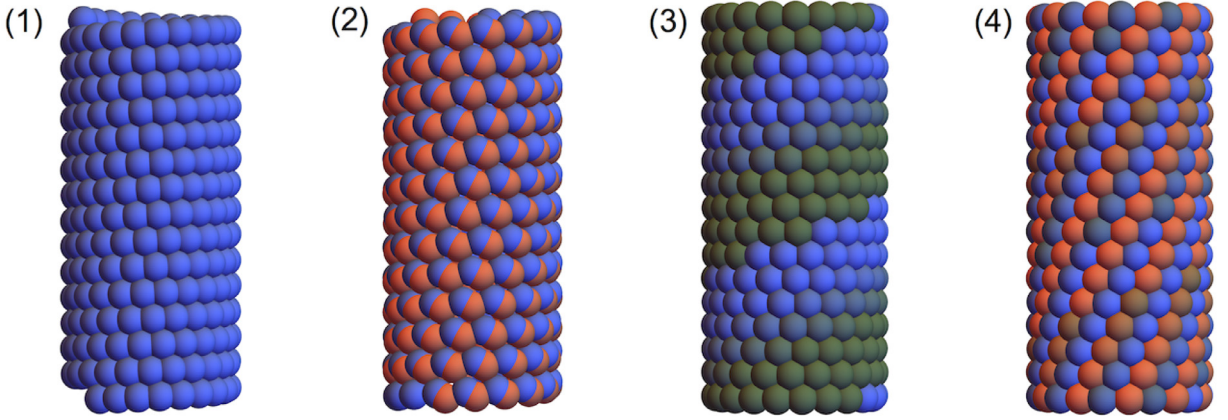
Fig. 1. Helical groups corresponding to (1)–(4), respectively. Each picture is the orbit of a single ball under the corresponding group and the coloring is according to the powers s or n.

terms of the group (3). We therefore focus on the largest collection of Abelian helical groups (3) below, as this contains all possible Abelian groups that can generate a helical structure.

Another reason for this focus is based on discrete notions of compatibility studied in Falk and James (2006) which suggest that compatibility is related fundamentally to Abelian groups. This concerns the interpretation of compatibility as relating to the process of returning to the same atom position by going around a loop in the space $\mathbb{Z}^2$ of powers of the group elements.

We note that incidentally our assumptions also include several rod groups. (Rod groups have periodicity along the axis through $\mathbf{e}$.) This is because we do not use the assumption that θ is an irrational multiple of 2π in any of the results below.

Consider the two phases a and b each described as orbits of a molecule under the general Abelian helical group (3). Assign group parameters $\theta_{a,b} \in \mathbb{R}$, $\alpha_{a,b} = 2\pi/i_{a,b}$, $i_{a,b} \in \mathbb{N} \setminus \{0\}$, $\tau_{a,b} \in \mathbb{R}$, $\mathbf{z}_{a,b} \in \mathbb{R}^3$ and $\mathbf{e}_{a,b} \in \mathbb{R}^3$, $|\mathbf{e}_{a,b}| = 1$. Define $\mathbf{Q}_\xi^{a,b} \in SO(3)$ having axis $\mathbf{e}_{a,b}$ and angle ξ, i.e.,

$$\mathbf{Q}_\xi^{a,b} = \sin\xi\, \mathbf{W}^{a,b} + \cos\xi\,(\mathbf{I} - \mathbf{e}_{a,b} \otimes \mathbf{e}_{a,b}) + \mathbf{e}_{a,b} \otimes \mathbf{e}_{a,b}, \tag{5}$$

respectively, where $\mathbf{W}^{a,b} = -\mathbf{W}^{a,b\ T} = -\mathbf{e}_1^{a,b} \otimes \mathbf{e}_2^{a,b} + \mathbf{e}_2^{a,b} \otimes \mathbf{e}_1^{a,b}$, where $\mathbf{e}_1^{a,b}, \mathbf{e}_2^{a,b}, \mathbf{e}_{a,b}$ is a right- orthonormal basis. From this hypothesis—in particular that $\mathbf{e}_a, \mathbf{e}_b$ do not depend on ξ—we also have that

$$\frac{d}{d\xi}\mathbf{Q}_\xi^a = \mathbf{Q}_\xi^a \mathbf{W}^a, \quad \frac{d}{d\xi}\mathbf{Q}_\xi^b = \mathbf{Q}_\xi^b \mathbf{W}^b. \tag{6}$$

Note that $\mathbf{Q}_\xi^{a,b}\mathbf{W}^{a,b} = \mathbf{W}^{a,b}\mathbf{Q}_\xi^{a,b}$, respectively. The two elements h^m and g^n can be combined and the group (3) can be written as

$$G_a = \left\{ \left(\mathbf{Q}_{m\theta_a + n\alpha_a}^a \,\middle|\, m\tau_a \mathbf{e}_a + (\mathbf{I} - \mathbf{Q}_{m\theta_a + n\alpha_a}^a)\mathbf{z}_a \right) : m \in \mathbb{Z}, \ n = 1, \dots, i_a \right\},$$

$$G_b = \left\{ \left(\mathbf{Q}_{m\theta_b + n\alpha_b}^b \,\middle|\, m\tau_b \mathbf{e}_b + (\mathbf{I} - \mathbf{Q}_{m\theta_b + n\alpha_b}^b)\mathbf{z}_b \right) : m \in \mathbb{Z}, \ n = 1, \dots, i_b \right\}, \tag{7}$$

with sub/superscripts a and b denoting the two phases. It can be seen from the formulas in (7) that $G_{a,b}$ are groups under the product rule for isometries given in the introduction, e.g.,

$$\left(\mathbf{Q}_{m\theta_a + n\alpha_a}^a \,\middle|\, m\tau_a \mathbf{e}_a + (\mathbf{I} - \mathbf{Q}_{m\theta_a + n\alpha_a}^a)\mathbf{z}_a \right)\left(\mathbf{Q}_{m'\theta_a + n'\alpha_a}^a \,\middle|\, m'\tau_a \mathbf{e}_a + (\mathbf{I} - \mathbf{Q}_{m'\theta_a + n'\alpha_a}^a)\mathbf{z}_a \right)$$

$$= \left(\mathbf{Q}_{(m+m')\theta_a + (n+n')\alpha_a}^a \,\middle|\, (m+m')\tau_a \mathbf{e}_a + (\mathbf{I} - \mathbf{Q}_{(m+m')\theta_a + (n+n')\alpha_a}^a)\mathbf{z}_a \right). \tag{8}$$

Note that if $(n + n') > i_a$, then $(n + n')$ in (8) can be replaced by $(n + n') \bmod i_a$.

The two groups G_a and G_b have different parameters. Our main task is to determine all choices of these parameters that give compatible interfaces.

These groups act on position vectors of atoms in one molecule as described above. For the purpose of studying compatibility we picture the molecule as reasonably compact and we discuss conditions of compatibility in terms of its center of mass. The precise statement of this assumption is that a typical diameter of the molecule is on the order of, or less than, the nearest neighbor distance between molecules defined in Section 3. The examples of helical structures given in the introduction (including the tail sheath of bacteriophage T4) have this property.
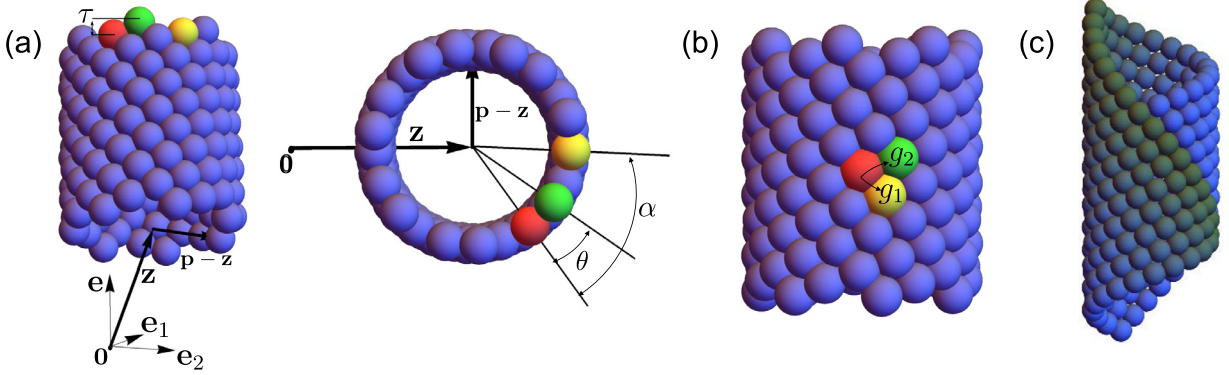
Fig. 2. (a) The structural parameters θ, α, τ, $\mathbf{p}$, $\mathbf{z}$, $\mathbf{e}$ for the original parameterization of the helical groups. For this example, $\theta = 0.34$, $\alpha = 2\pi/7$, $\tau = 0.12$, $\mathbf{p} = (2,1,2)$, $\mathbf{z} = (2,0,2)$, $\mathbf{e} = (0,0,1)$. (b) Reparameterization of the group by the nearest neighbor generators found by the algorithm (see text). Red is mapped to yellow by g_1 and red is mapped to green by g_2. (c) Calculation of the domain $\mathcal{D}$. In this case $q^* = 14$ and the shading is according to the value of q. (For interpretation of the references to color in this figure legend, the reader is referred to the web version of this article.)

The helical structures a and b consist of atomic positions given by the corresponding groups each acting on its respective center-of-mass position $\mathbf{p}_{a,b}$. Therefore, the center-of-mass positions of the helical structures are given by

$$\mathbf{y}_a(n, m) = \mathbf{Q}^a_{m\theta_a + n\alpha_a}(\mathbf{p}_a - \mathbf{z}_a) + m\tau_a\mathbf{e}_a + \mathbf{z}_a, \ \ m \in \mathbb{Z}, \ \ n = 1, \ldots, i_a,$$
$$\mathbf{y}_b(n, m) = \mathbf{Q}^b_{m\theta_b + n\alpha_b}(\mathbf{p}_b - \mathbf{z}_b) + m\tau_b\mathbf{e}_b + \mathbf{z}_b, \ \ m \in \mathbb{Z}, \ \ n = 1, \ldots, i_b. \tag{9}$$

In the language of objective structures the structure a as viewed from the center of mass position $\mathbf{y}_a(m, n)$ is exactly the same as the structure viewed from $\mathbf{y}_a(m', n')$, for any choices of the integers m, n, m', n' (even though there may be no atoms at these centers of mass). Dropping off the subscripts, we define θ, α, τ, $\mathbf{p}$, $\mathbf{z}$, $\mathbf{e}$ in (9) as the *structural parameters* for the helical structure. These parameters are illustrated in Fig. 2(a) for a particular example.

3. Nearest-neighbor reparameterization of the groups

In this section, we describe a reparameterization of the helical groups that lends itself naturally to the study of compatible interfaces between phases. To set the notation, we drop the superscripts a, b and consider a single helical group G defined as above by

$$G = \{g(n, m) : m \in \mathbb{Z}, \ n = -i, \ldots, 0, \ldots, i\}, \quad g(n, m) = \left(\mathbf{Q}_{m\theta + n\alpha} \ \middle| \ m\tau\mathbf{e} + (\mathbf{I} - \mathbf{Q}_{m\theta + n\alpha})\mathbf{z}\right). \tag{10}$$

Here, we have extended the domain of integers for n to include $-i, -i+1, \ldots, 0$ for technical reasons. All this does is simply count some group elements more than once, which does not change G (the collection of all such elements). As before, let the atomic positions be given by $\mathbf{y}(n, m) = g(n, m)(\mathbf{p})$. We assume without loss of generality that, $\mathbf{p} - \mathbf{z} \neq 0$, $(\mathbf{p} - \mathbf{z}) \cdot \mathbf{e} = 0$, $\tau \neq 0$ to avoid degenerate structures (lines, rings). Note that $g(0, 0) = id$, so that $\mathbf{y}(0, 0) = \mathbf{p}$.

Conditions of compatibility between phases ensure that nearby atoms before transformation remain near each other after transformation. Thus, distances are important. However, the standard parameterization of the groups given above in terms of n and m does not in general have the property that if $\mathbf{y}(n, m)$ is near $\mathbf{y}(n', m')$ in $\mathbb{R}^3$, then (n, m) is near (n', m') in $\mathbb{Z}^2$ (for instance, the example in Fig. 2(a)). Therefore, it is desirable to reparameterize the groups so that nearest and next-to-nearest neighbors of any point $\tilde{\mathbf{y}}(p, q)$ are $\tilde{\mathbf{y}}(p + 1, q)$, $\tilde{\mathbf{y}}(p, q + 1)$. Here $\tilde{\mathbf{y}}(p, q)$ is the deformation induced by a new parameterization of the group. Because G is an isometry group (i.e., preserves distances), we then have at least four nearest and next-to-nearest neighbors with positions $\tilde{\mathbf{y}}(p + 1, q)$, $\tilde{\mathbf{y}}(p - 1, q)$, $\tilde{\mathbf{y}}(p, q + 1)$, $\tilde{\mathbf{y}}(p, q - 1)$. (Of course, there may be additional nearest, or next-to-nearest, neighbors such as the case when $\tilde{\mathbf{y}}(n, m)$ is surrounded by six nearest neighbors.) We show in the appendix that, under mild assumptions on the group parameters, it is always possible to find such nearest neighbor generators.

We collect these results in the form of an algorithm.

Algorithm: nearest neighbor generators. *Let G be given by (10) with group parameters $\tau \neq 0$, $\alpha = 2\pi/i$, $i \in \mathbb{N} \setminus \{0\}$, and let $r = |\mathbf{p} - \mathbf{z}| > 0$, $(\mathbf{p} - \mathbf{z}) \cdot \mathbf{e} = 0$, the unit vector $\mathbf{e}$ being on the axis of $\mathbf{Q}_{(\cdot)}$. Let (n_1, m_1) be a minimizer of the finite-dimensional minimization problem,*

$$\min_{\substack{n \in \{-i, \ldots, 0, \ldots, i\} \\ m \in \mathbb{Z} \cap [-h, h]}} 4r^2 \sin^2\left(\frac{m\theta + n\alpha}{2}\right) + m^2\tau^2, \tag{11}$$

and let (n_2, m_2) be a minimizer of (11) subject to the constraint $m_1 n \neq m n_1$. Here, h is the smallest integer greater than $2r^2/\tau^2 - 1/2$.

These minimizers always exist. Further, if $-\pi/2 \leq m_1\theta + n_1\alpha \leq \pi/2$ and $-\pi/2 \leq m_2\theta + n_2\alpha \leq \pi/2$, then nearest neighbor generators of G are given by

$$g_1 = g(n_1, m_1), \quad g_2 = g(n_2, m_2). \tag{12}$$

This parameterization has the following properties:

- *The group satisfies $G = \{g_1^p g_2^q : (p, q) \in \mathbb{Z}^2\}$;*
- *The deformation $\tilde{\mathbf{y}}(p, q) = g_1^p g_2^q(\mathbf{p})$ generates the same helical structure as the deformation $\mathbf{y}(n, m)$ above;*
- *$\tilde{\mathbf{y}}$ also maps neighbors on $\mathbb{Z}^2$ to neighbors on the helical structure, i.e., it has the additional property that $\tilde{\mathbf{y}}(p \pm 1, q)$ and $\tilde{\mathbf{y}}(p, q \pm 1)$ are nearest and next-to-nearest neighbors to $\tilde{\mathbf{y}}(p, q)$ on the structure* (Fig. 2(b)).

In other words, this procedure provides an explicit nearest neighbor parameterization for *any* Abelian group that generates a helical structure (i.e., those groups in (1) or (3)), as long as the parameters are such that the distance between neighboring atoms is sufficiently small compared to the radius of the cylinder. In particular, the parameterization of G consists of powers of the two nearest neighbor generators g_1 and g_2.

As it happens, arbitrary powers of g_1, g_2 give infinitely many pairs of powers that describe the same atom. We will have to reconcile this, as a group for generating a helical structure should not have repeated elements[6] since we want one an only one atom at each point in the orbit. To understand the issue, let the nearest neighbor generators $g_1 = g(n_1, m_1)$ and $g_2 = g(n_2, m_2)$ be given as above so that $m_1 n_2 \neq m_2 n_1$ with $n_1, n_2 \in \{-i, \ldots, 0, \ldots, i\}$. We claim that there are always values $(p, q) \neq (0, 0)$ such that $g_1^p g_2^q = id$. Indeed, under our hypotheses, these are those $(p, q) \in \mathbb{Z}^2$ satisfying

$$pn_1 + qn_2 = ni, \quad pm_1 + qm_2 = 0 \tag{13}$$

for some $n \in \mathbb{Z}$. Since $n_1 m_2 - n_2 m_1 \neq 0$, the solutions of this system are pairs of integers (p, q) satisfying

$$p = ni\left(\frac{m_2}{n_1 m_2 - n_2 m_1}\right), \quad q = ni\left(\frac{-m_1}{n_1 m_2 - n_2 m_1}\right). \tag{14}$$

There are infinitely many such solutions since $n \in \mathbb{Z}$ can be freely chosen. (Note, every $n = k(n_1 m_2 - n_2 m_1)$ for $k \in \mathbb{Z}$ gives such a pair of integers.) In the appendix, we derive a general procedure for finding a suitable domain of these powers that specifies the group G completely and has no repeated elements. The general idea is sketched in Fig. 2(c).

We also collect these results in the form of an algorithm.

Algorithm: domain of powers of the generators. *Assume the conditions on parameters listed above for the derivation of nearest neighbor generators, and choose the labeling of the generators g_1 and g_2 so that $m_1 \neq 0$. Let $\hat{q}(n) = -ni m_1/(n_1 m_2 - n_2 m_1)$ and define*

$$q^\star = \min_{\substack{n \in \mathbb{Z} \setminus \{0\} \\ \hat{q}(n) > 0 \\ \hat{q}(n) \in \mathbb{Z}}} \hat{q}(n). \tag{15}$$

Then for any $q_0 \in \mathbb{Z}$, $\mathcal{D}_{q_0} = (0, q_0) + \mathcal{D} = \mathbb{Z} \times \{q_0 + 1, \ldots, q_0 + q^\star\}$ has the property that $G = \{g_1^p g_2^q : (p, q) \in \mathcal{D}_{q_0}\}$, and this description has no repeated elements.

4. Discrete vs. continuum concepts of compatibility

Compatibility in discrete structures is fundamentally connected with Abelian groups. It concerns the fact that a product of group elements that corresponds to a loop in the space of powers $\mathbb{Z}^n$ of the n generators gives the identity. When the group is the infinitesimal translation group operating on $\mathbb{R}^n$ and the action of the group on vector fields $\mathbf{v}(\mathbf{p}), \mathbf{p} \in \mathbb{R}^n$ is arranged appropriately, this gives the usual notion of calculus, i.e., conditions under which $\mathbf{v} = \nabla\varphi$. Another example is given in Falk and James (2006) in which molecules interact according to their positions and orientations.

As far as we are aware, there is no theory of compatibility for interfaces between atomistic phases having different sets of structural parameters. This would involve the formulation of appropriate definitions that say that one can set up a correspondence of neighboring molecules, such that corresponding molecules before transformation remain close after partial transformation, when separated by a phase boundary.

On the other hand, there is a straightforward and simple notion of compatibility at interfaces for discrete structures that is directly inherited from continuum ideas. In the present case it is the following. After passing to nearest neighbor parameterization as above, we consider the formulas $\mathbf{y}_{a,b}(p, q)$ induced by this parameterization. The functions $\mathbf{y}_a(p, q)$ and $\mathbf{y}_b(p, q)$ are defined on different discrete domains, but they make perfect sense if they are extended to a suitable strip in $\mathbb{R}^2$. We wish to use continuity of these functions to impose compatibility, and for this purpose we will extend their domains to all values of $(p, q) \in \mathbb{R} \times (0, q^\star_{a,b}] \subset \mathbb{R}^2$. (For simplicity we take $q_0 = 0$.) Restrict the structure a to be locally on one side of an interface $(p, q) = (\hat{p}(s), \hat{q}(s))$, $s_1 < s < s_2$ and b to be on the other side. Then, under suitable smoothness assumptions, the standard continuum notion of compatibility is

$$\nabla_{p,q}\mathbf{y}_a(\hat{p}(s), \hat{q}(s)) - \nabla_{p,q}\mathbf{y}_b(\hat{p}(s), \hat{q}(s)) = \mathbf{a}(s) \otimes \mathbf{n}(s), \quad \mathbf{n}(s) = (-\hat{q}'(s), \hat{p}'(s)); \tag{16}$$

---

[6] In general, group theory assumes an indexing with no repeated elements.

that is, equivalently,

$$\big(\partial_p \mathbf{y}_a(\hat{p}(s), \hat{q}(s)) - \partial_p \mathbf{y}_b(\hat{p}(s), \hat{q}(s))\big)\hat{p}'(s) + \big(\partial_q \mathbf{y}_a(\hat{p}(s), \hat{q}(s)) - \partial_q \mathbf{y}_b(\hat{p}(s), \hat{q}(s))\big)\hat{q}'(s) = 0. \tag{17}$$

Note that there is a lot of freedom here. Even with this canonical interpolation, we have complete freedom on where to place the interface $(\hat{p}(s), \hat{q}(s))$ between the discrete positions. In this paper we define compatibility by using (17).

Note that we use the same interface $(\hat{p}(s), \hat{q}(s))$ in the reference domain for both structures in $\mathbb{R}^2$. This also does not seem to be restrictive, since we allow the group parameters as well as the $(0,0)$ positions to be assignable. However, the interface has to respect the two (potentially different) periods $q_a^\star$ and $q_b^\star$. If, say, $q_a^\star < q_b^\star$ and the interface extends into the region $q_a^\star < q < q_b^\star$ then $\mathbf{y}_a$ is undefined on this region: there are no molecules from structure a that can be matched with those of b across this part of the interface. Thus we assume $0 < \hat{q}(s) \leq \min\{q_a^\star, q_b^\star\}$. Moreover, we solve rigorously the local problem: under mild hypotheses we find necessary and sufficient conditions that (17) is satisfied in a sufficiently small neighborhood $s_1 < s < s_2$ on which $0 < \hat{q}(s) \leq \min\{q_a^\star, q_b^\star\}$. Then we show that some of these solutions can be extended to larger intervals.

5. Local compatibility for nearest neighbor generators

Hypotheses on the groups. Let $G_a \neq G_b$ be the two helical groups

$$G_a = \left\{ \left(\mathbf{Q}_{m\theta_a + n\alpha_a}^a \,\middle|\, m\tau_a \mathbf{e}_a + (\mathbf{I} - \mathbf{Q}_{m\theta_a + n\alpha_a}^a)\mathbf{z}_a \right) : m \in \mathbb{Z}, \ n = 1, \ldots, i_a \right\},$$

$$G_b = \left\{ \left(\mathbf{Q}_{m\theta_b + n\alpha_b}^b \,\middle|\, m\tau_b \mathbf{e}_b + (\mathbf{I} - \mathbf{Q}_{m\theta_b + n\alpha_b}^b)\mathbf{z}_b \right) : m \in \mathbb{Z}, \ n = 1, \ldots, i_b \right\}, \tag{18}$$

where $\mathbf{z}_{a,b}, \mathbf{e}_{a,b} \in \mathbb{R}^3$, the unit vector $\mathbf{e}_{a,b}$ being on the axis of $\mathbf{Q}_{(.)}^{a,b} \in SO(3)$, and $\tau_{a,b} \neq 0, \theta_{a,b} \in \mathbb{R}, \alpha_{a,b} = 2\pi/i_{a,b}, i_{a,b} \in \mathbb{N}$. The helical structures are generated by applying these groups on $\mathbf{p}_{a,b} \in \mathbb{R}^3$ with $r_{a,b} = |\mathbf{p}_{a,b} - \mathbf{z}_{a,b}| > 0$, $(\mathbf{p}_{a,b} - \mathbf{z}_{a,b}) \cdot \mathbf{e}_{a,b} = 0$. Nearest neighbor generators given by (11) and (15) generate the re-parameterized groups

$$G_a = \left\{ \left(\mathbf{Q}_{p\psi_a + q\beta_a}^a \,\middle|\, (pm_1^a + qm_2^a)\tau_a \mathbf{e}_a + (\mathbf{I} - \mathbf{Q}_{p\psi_a + q\beta_a}^a)\mathbf{z}_a \right) : p \in \mathbb{Z}, \ q = 1, \ldots, q_a^\star \right\},$$

$$G_b = \left\{ \left(\mathbf{Q}_{p\psi_b + q\beta_b}^b \,\middle|\, (pm_1^b + qm_2^b)\tau_b \mathbf{e}_b + (\mathbf{I} - \mathbf{Q}_{p\psi_b + q\beta_b}^b)\mathbf{z}_b \right) : p \in \mathbb{Z}, \ q = 1, \ldots, q_b^\star \right\} \tag{19}$$

with no repeated elements. Here $\psi_{a,b} = m_1^{a,b}\theta_{a,b} + n_1^{a,b}\alpha_{a,b}, \beta_{a,b} = m_2^{a,b}\theta_{a,b} + n_2^{a,b}\alpha_{a,b}$, and, to satisfy the algorithms for construction of the nearest neighbor generators, the integers $m_1^{a,b}$ and $m_2^{a,b}$ satisfy the condition $m_1^{a,b}n_2^{a,b} \neq m_2^{a,b}n_1^{a,b}$. The latter is equivalent to $m_2^{a,b}\psi_{a,b} \neq m_1^{a,b}\beta_{a,b}$ and $-\pi/2 \leq \psi_{a,b}, \beta_{a,b} \leq \pi/2$.

Hypotheses on the interface, compatibility and orientability. The two helical structures generated by (19) are

$$\mathbf{y}_a(p, q) = \mathbf{Q}_{p\psi_a + q\beta_a}^a \mathbf{r}_a + (pm_1^a + qm_2^a)\tau_a \mathbf{e}_a + \mathbf{z}_a, \ p \in \mathbb{Z}, \ q = 1, \ldots, q_a^\star,$$

$$\mathbf{y}_b(p, q) = \mathbf{Q}_{p\psi_b + q\beta_b}^b \mathbf{r}_b + (pm_1^b + qm_2^b)\tau_b \mathbf{e}_b + \mathbf{z}_b, \quad p \in \mathbb{Z}, \ q = 1, \ldots, q_b^\star, \tag{20}$$

where $\mathbf{r}_{a,b} = \mathbf{p}_{a,b} - \mathbf{z}_{a,b}, \mathbf{r}_{a,b} \cdot \mathbf{e}_{a,b} = 0$. Following the discussion of Section 4, we extend the domain of $\mathbf{y}_{a,b}(p, q)$ to a suitable subset of $\mathbb{R}^2$, and we seek an arclength parameterized twice continuously differentiable curve $(\hat{p}(s), \hat{q}(s)) \in \mathbb{R}^2$ defined on $s_1 < s < s_2$ and satisfying $0 \leq \hat{q}(s) \leq \min\{q_a^\star, q_b^\star\}$, $\hat{p}'(s)^2 + \hat{q}'(s)^2 = 1$. The condition that the interface can be parameterized by arclength is without loss of generality, since the condition (17) is linear in $\hat{p}', \hat{q}'$. The *local compatibility condition* is then given by

$$\hat{p}'(s)\Big(\mathbf{Q}_{\hat{p}(s)\psi_a + \hat{q}(s)\beta_a}^a(\psi_a \mathbf{W}^a \mathbf{r}_a + m_1^a \tau_a \mathbf{e}_a) - \mathbf{Q}_{\hat{p}(s)\psi_b + \hat{q}(s)\beta_b}^b(\psi_b \mathbf{W}^b \mathbf{r}_b + m_1^b \tau_b \mathbf{e}_b)\Big)$$

$$= -\hat{q}'(s)\Big(\mathbf{Q}_{\hat{p}(s)\psi_a + \hat{q}(s)\beta_a}^a(\beta_a \mathbf{W}^a \mathbf{r}_a + m_2^a \tau_a \mathbf{e}_a) - \mathbf{Q}_{\hat{p}(s)\psi_b + \hat{q}(s)\beta_b}^b(\beta_b \mathbf{W}^b \mathbf{r}_b + m_2^b \tau_b \mathbf{e}_b)\Big), \tag{21}$$

for $s \in (s_1, s_2)$ and with the hypotheses on the parameters given above. We obtained this formula simply by substituting (20) into (17).

Below, we identify necessary and sufficient conditions on structural parameters $\{\psi_{a,b}, \beta_{a,b}, \tau_{a,b} \in \mathbb{R}; \mathbf{r}_{a,b}, \mathbf{z}_{a,b}, \mathbf{e}_{a,b} \in \mathbb{R}^3, |\mathbf{e}_{a,b}| = 1; m_1^{a,b}, m_2^{a,b} \in \mathbb{Z}\}$ satisfying the restrictions given above that allow for the existence of such curves. Note that we allow the full set of parameters to vary, so that the two helical phases can lie on different cylinders of arbitrary positive radius, with arbitrary orientation, and lying on arbitrary axes. Further, the structural parameters defining pitch and other characteristics are subject to only very mild restrictions.

We also note that we have not specified that the two mappings $\mathbf{y}_a$ and $\mathbf{y}_b$ map points on opposite sides of the interface on the reference domain to opposite sides of the interface on the cylinder. That is, in a sufficiently small neighborhood $\mathcal{D} = \mathcal{D}^+ \cup \mathcal{D}^- \subset \mathbb{R} \times (0, q^\star)$ of a point $(\hat{p}(s_0), \hat{q}(s_0))$ divided by the interface into disjoint regions $\mathcal{D}^+$ and $\mathcal{D}^-$, we may have the situation that compatible deformations $\mathbf{y}_a(\mathcal{D}^-)$ and $\mathbf{y}_b(\mathcal{D}^+)$ map to overlapping regions on the cylinder. In this case we consider helical structures given by $\mathbf{y}_a(\mathcal{D}^-) \cup \mathbf{y}_b(\mathcal{D}^-)$ (or $\mathbf{y}_a(\mathcal{D}^+) \cup \mathbf{y}_b(\mathcal{D}^+)$). This is consistent with the idea that

nanotubes are not typically synthesized by deformations of a flat sheet of atoms, i.e, the functions (20) do not represent actual deformations, but just parameterizations. The condition of compatibility is still reasonable in this case in that a point $(p, q) \in \mathbb{Z}^2 \cap \mathcal{D}^-$ near the interface is mapped by $\mathbf{y}_a$ and $\mathbf{y}_b$ to a nearby point on the cylinder by compatibility, and so one can set up a 1-1 correspondence of nearby points of the two phases.

However, it is useful for the comparison with the "rolling-up construction" (Dumitrică and James, 2007) (disallowing folding), and for our analysis of slips and twins in Section 7, to distinguish the two cases. Therefore we will say that the parameterization of a compatible interface is *orientable* if

$$(\mathbf{y}_{a,p} \times \mathbf{y}_{a,q}) \cdot (\mathbf{y}_{b,p} \times \mathbf{y}_{b,q}) > 0 \quad \text{on } (\hat{p}(s), \hat{q}(s)), \quad s_1 < s < s_2. \tag{22}$$

We introduce the vectors

$$\mathbf{f}_{a,b} = \begin{pmatrix} \psi_{a,b} \\ \beta_{a,b} \end{pmatrix}, \quad \mathbf{g}_{a,b} = \tau_{a,b} \begin{pmatrix} m_1^{a,b} \\ m_2^{a,b} \end{pmatrix} \tag{23}$$

in order to consolidate the parameters. In terms of $\mathbf{f}_{a,b} \in [-\pi/2, \pi/2] \times [-\pi/2, \pi/2]$, $\mathbf{g}_{a,b} \in \mathbb{R}^2$ and $\mathbf{x}(s) = (\hat{p}(s), \hat{q}(s))$ the formulas (20) give an explicit form of the condition (22) for an orientable interface:

$$(\mathbf{y}_{a,p} \times \mathbf{y}_{a,q}) \cdot (\mathbf{y}_{b,p} \times \mathbf{y}_{b,q})(s) = (\mathbf{f}_a \cdot \mathbf{g}_a^\perp)(\mathbf{f}_b \cdot \mathbf{g}_b^\perp)(\mathbf{Q}_{\mathbf{f}_a \cdot \mathbf{x}(s)}^a \mathbf{r}_a \cdot \mathbf{Q}_{\mathbf{f}_b, \mathbf{x}(s)}^b \mathbf{r}_b) > 0, \tag{24}$$

where we use the standard notation that $\perp$ denotes a counterclockwise rotation about the axis perpendicular to the plane by $\pi/2$, e.g., $\mathbf{f}_{a,b}^\perp = (-\beta_{a,b}, \psi_{a,b})$ and $\mathbf{g}_{a,b}^\perp = \tau_{a,b}(-m_2^{a,b}, m_1^{a,b})$.

Simplification of the local compatibility condition. The compatibility condition (21) can be simplified. To do this, we first consolidate some of the notation.

As just above, we set $\mathbf{x}(s) = (\hat{p}(s), \hat{q}(s))$ for the arc-length parameterized curves. Thus, we have $|\mathbf{x}'(s)| = 1$ for all $s \in (s_1, s_2)$, and so we define

$$\mathbf{t}(s) = \mathbf{x}'(s), \quad \mathbf{n}(s) = \mathbf{t}(s)^\perp = \begin{pmatrix} -\hat{q}'(s) \\ \hat{p}'(s) \end{pmatrix}. \tag{25}$$

The tangent $\mathbf{t}(s)$ to the interface and normal $\mathbf{n}(s)$ forms an orthonormal basis at each point $\mathbf{x}(s)$, and

$$\mathbf{t}'(s) = \kappa(s)\mathbf{n}(s), \quad s_1 < s < s_2, \tag{26}$$

where $\kappa(s) \in \mathbb{R}$ gives the *curvature* of the interface at each $\mathbf{x}(s)$. The nondegeneracy conditions $m_2^{a,b}\psi_{a,b} \neq m_1^{a,b}\beta_{a,b}$ we have assumed above on group parameters are:

$$\mathbf{f}_{a,b} \cdot \mathbf{g}_{a,b}^\perp \neq 0, \quad \mathbf{g}_{a,b} \cdot \mathbf{h} = 0 \quad \text{for some} \quad \mathbf{h} \in \mathbb{Z}^2 \setminus \{\mathbf{0}\}. \tag{27}$$

We take these conditions to hold throughout.

The local compatibility equation can now be written as a total derivative,

$$\left(\mathbf{Q}_{\mathbf{x}(s) \cdot \mathbf{f}_a}^a \mathbf{r}_a + (\mathbf{x}(s) \cdot \mathbf{g}_a)\mathbf{e}_a\right)' = \left(\mathbf{Q}_{\mathbf{x}(s) \cdot \mathbf{f}_b}^b \mathbf{r}_b + (\mathbf{x}(s) \cdot \mathbf{g}_b)\mathbf{e}_b\right)' \tag{28}$$

for $s \in (s_1, s_2)$.

We can catalogue all ways of obtaining a locally compatible interface based on properties of the parameterized interface $\mathbf{x}(s)$ (see (25) and (26)). First note that either $\mathbf{t}(s) = \mathbf{t} = const.$ on (s_1, s_2) or there is a point $s^* \in (s_1, s_2)$ where the curvature is nonzero. In the latter case, since we are solving the local problem, we shrink the interval $(s_1, s_2), s_1 < s^* < s_2$ so that $\kappa(s) \neq 0$ on (s_1, s_2). Thus, for the *locally compatible interface* there are two cases to consider:

1. $\mathbf{t}(s) = \mathbf{t} = const.$ for all $s \in (s_1, s_2)$.
2. The curvature $\kappa(s) \neq 0$ for all $s \in (s_1, s_2)$.

In the remainder of this section, we develop a complete characterization of local compatibility. We state this characterization in the form of theorems for each of the two cases above. These results are then summarized and discussed in the next section.

5.1. Implications of vanishing interface curvature

Lemma 5.1. *Assume the hypotheses on the helical groups $G_a \neq G_b$ and on the interface. The curvature $\kappa(s) = 0$ for all $s \in (s_1, s_2)$ if and only if the cylinders are parallel, $\mathbf{e}_a \times \mathbf{e}_b = 0$.*

Proof. ($\Leftarrow$) Without loss of generality, we can assume $\mathbf{e}_a = \mathbf{e}_b = \mathbf{e}$ since the case $\mathbf{e}_a = -\mathbf{e}_b$ has an identical structure (after replacing $\mathbf{f}_a$ with $-\mathbf{f}_a$ and $\mathbf{g}_a$ with $-\mathbf{g}_a$). After explicit differentiation and some rearranging of terms, (28) becomes

$$(\mathbf{t}(s) \cdot \mathbf{f}_a)\mathbf{Q}_{\mathbf{x}(s) \cdot \mathbf{f}_a}\mathbf{W}\mathbf{r}_a - (\mathbf{t}(s) \cdot \mathbf{f}_b)\mathbf{Q}_{\mathbf{x}(s) \cdot \mathbf{f}_b}\mathbf{W}\mathbf{r}_b = ((\mathbf{g}_b - \mathbf{g}_a) \cdot \mathbf{t}(s))\mathbf{e} \tag{29}$$

for $s \in (s_1, s_2)$. Here, $\mathbf{Q}_{(\cdot)} = \mathbf{Q}_{(\cdot)}^a = \mathbf{Q}_{(\cdot)}^b$ and $\mathbf{W} = \mathbf{W}^a = \mathbf{W}^b$ since $\mathbf{e}_{a,b} = \mathbf{e}$ (recall (5)). Both $\mathbf{Q}_{\mathbf{x}(s) \cdot \mathbf{f}_b}\mathbf{W}\mathbf{r}_b$ and $\mathbf{Q}_{\mathbf{x}(s) \cdot \mathbf{f}_a}\mathbf{W}\mathbf{r}_a$ are perpendicular to $\mathbf{e} = \mathbf{e}_{a,b}$. Thus, equality holds if and only if both sides vanish. For the right-hand side, $(\mathbf{g}_b - \mathbf{g}_a) \cdot \mathbf{t}(s) = 0$. By

differentiating this identity, we have that $\kappa(s)(\mathbf{g}_b - \mathbf{g}_a) \cdot \mathbf{n}(s) = 0$. Since $\mathbf{n}(s)$ is perpendicular to $\mathbf{t}(s)$, we conclude $\kappa(s) = 0$ for all $s \in (s_1, s_2)$, or $\mathbf{g}_a = \mathbf{g}_b$. If the latter condition *does not* hold, then the proof is complete. Hence, we assume $\mathbf{g}_a = \mathbf{g}_b$.

Substituting $\mathbf{g}_a = \mathbf{g}_b$ back into (29), the left-hand side vanishes. There are then two distinct cases to consider:

(a) The vectors $\mathbf{Q}_{\mathbf{x}(s) \cdot \mathbf{f}_b} \mathbf{W} \mathbf{r}_b$ and $\mathbf{Q}_{\mathbf{x}(s) \cdot \mathbf{f}_a} \mathbf{W} \mathbf{r}_a$ are parallel for all $s \in (s_1, s_2)$.
(b) These vectors are linearly independent on some interval[7] $(\tilde{s}_1, \tilde{s}_2) \subset (s_1, s_2)$.

We suppose (a). Then, we can write $\mathbf{Q}_{\mathbf{x}(s) \cdot \mathbf{f}_a} \mathbf{W} \mathbf{r}_a = \pm(|\mathbf{r}_a|/|\mathbf{r}_b|) \mathbf{Q}_{\mathbf{x}(s) \cdot \mathbf{f}_b} \mathbf{W} \mathbf{r}_b$, where the $\pm$ is fixed for all s (given the smoothness hypothesis). This implies $\mathbf{W} \mathbf{r}_a = \pm(|\mathbf{r}_a|/|\mathbf{r}_b|) \mathbf{Q}_{\mathbf{x}(s) \cdot (\mathbf{f}_b - \mathbf{f}_a)} \mathbf{W} \mathbf{r}_b$ since $\mathbf{e}_{a,b} = \mathbf{e}$. By differentiating this quantity, we deduce the identity $\mathbf{t}(s) \cdot (\mathbf{f}_b - \mathbf{f}_a) = 0$. By differentiating this, we deduce that either $\kappa(s) = 0$ for all s or $\mathbf{f}_b = \mathbf{f}_a$. We assume the latter, as the former is desired. In substituting this back into (29) (using that $\mathbf{g}_a = \mathbf{g}_b$ and $\mathbf{f}_a = \mathbf{f}_b \neq 0$), we conclude $\mathbf{r}_a = \mathbf{r}_b$ since $\mathbf{Q}_{\mathbf{x}(s) \cdot (\mathbf{f}_b - \mathbf{f}_a)} = \mathbf{I}$. But then, $\mathbf{g}_a = \mathbf{g}_b$, $\mathbf{f}_a = \mathbf{f}_b$ and $\mathbf{r}_a = \mathbf{r}_b$, violating the hypothesis $G_a \neq G_b$.

We suppose (b). Then, $\mathbf{Q}_{\mathbf{x}(s) \cdot \mathbf{f}_b} \mathbf{W} \mathbf{r}_b$ and $\mathbf{Q}_{\mathbf{x}(s) \cdot \mathbf{f}_a} \mathbf{W} \mathbf{r}_a$ are linearly independent for all $s \in (\tilde{s}_1, \tilde{s}_2)$. Consequently, the left-hand side of (29) vanishes on this interval if and only if $\mathbf{t}(s) \cdot \mathbf{f}_b = \mathbf{t}(s) \cdot \mathbf{f}_a = 0$ for all $s \in (\tilde{s}_1, \tilde{s}_2)$. By differentiating these identities (as we did above), we conclude that either $\kappa(s) = 0$ for $s \in (\tilde{s}_1, \tilde{s}_2)$ or $\mathbf{f}_a = \mathbf{f}_b = 0$. The latter contradicts the hypotheses on the group parameters stated at the start of this section. So the former must be true in this case.

In summary, we have shown that $(\mathbf{e}_a \times \mathbf{e}_b) = 0$ implies $\kappa(s) = 0$ for all $s_1 < s < s_2$, in both cases (a) and (b).

($\Rightarrow$) Suppose, for the sake of a contradiction, that $\kappa(s) = 0$ for all $s \in (s_1, s_2)$ but $(\mathbf{e}_a \times \mathbf{e}_b) \neq 0$. By explicitly differentiating the compatibility condition in (28), we obtain

$$(\mathbf{t} \cdot \mathbf{f}_b) \mathbf{Q}^b_{\mathbf{x}(s) \cdot \mathbf{f}_b} \mathbf{W}^b \mathbf{r}_b - (\mathbf{t} \cdot \mathbf{f}_a) \mathbf{Q}^a_{\mathbf{x}(s) \cdot \mathbf{f}_a} \mathbf{W}^a \mathbf{r}_a = (\mathbf{g}_a \cdot \mathbf{t}) \mathbf{e}_a - (\mathbf{g}_b \cdot \mathbf{t}) \mathbf{e}_b \tag{30}$$

for all $s \in (s_1, s_2)$. Notice that the tangent $\mathbf{t}(s) = \mathbf{t} = const$ in this case. Thus, by differentiating twice more, we obtain two additional equations

$$(\mathbf{t} \cdot \mathbf{f}_b)^2 \mathbf{Q}^b_{\mathbf{x}(s) \cdot \mathbf{f}_b} \mathbf{r}_b = (\mathbf{t} \cdot \mathbf{f}_a)^2 \mathbf{Q}^a_{\mathbf{x}(s) \cdot \mathbf{f}_a} \mathbf{r}_a,$$
$$(\mathbf{t} \cdot \mathbf{f}_b)^3 \mathbf{Q}^b_{\mathbf{x}(s) \cdot \mathbf{f}_b} \mathbf{W}^b \mathbf{r}_b = (\mathbf{t} \cdot \mathbf{f}_a)^3 \mathbf{Q}^a_{\mathbf{x}(s) \cdot \mathbf{f}_a} \mathbf{W}^a \mathbf{r}_a, \tag{31}$$

which must hold for all $s \in (s_1, s_2)$. We dot both of these equations with $\mathbf{e}_b$ so that the left-hand sides vanish. Then, we must have $\mathbf{t} \cdot \mathbf{f}_a = 0$ or $\mathbf{e}_b \cdot \mathbf{Q}^a_{\mathbf{x}(s) \cdot \mathbf{f}_a} \mathbf{W}^a \mathbf{r}_a = \mathbf{e}_b \cdot \mathbf{Q}^a_{\mathbf{x}(s) \cdot \mathbf{f}_a} \mathbf{r}_a = 0$. However, the latter implies that $\mathbf{e}_b$ is parallel to $\mathbf{e}_a$ since the set $\{\mathbf{Q}^a_{\mathbf{x}(s) \cdot \mathbf{f}_a} \mathbf{r}_a, \mathbf{Q}^a_{\mathbf{x}(s) \cdot \mathbf{f}_a} \mathbf{W}^a \mathbf{r}_a, \mathbf{e}_a\}$ forms an orthogonal basis of $\mathbb{R}^3$. But $\mathbf{e}_a \times \mathbf{e}_b \neq 0$ by hypothesis. So we conclude $\mathbf{f}_a \cdot \mathbf{t} = 0$. Now, we instead dot the equations in (31) with $\mathbf{e}_a$ so that the right-hand sides vanish. By a similar argument, we conclude $\mathbf{f}_b \cdot \mathbf{t} = 0$. Substituting $\mathbf{f}_{a,b} \cdot \mathbf{t} = 0$ back into (30), we see that the left-hand side vanishes. It, therefore, follows that $\mathbf{g}_a \cdot \mathbf{t} = \mathbf{g}_b \cdot \mathbf{t} = 0$ since $\mathbf{e}_a \times \mathbf{e}_b \neq 0$. In summary, we have deduced that $\mathbf{f}_{a,b}$ and $\mathbf{g}_{a,b}$ are all parallel for this case. But this means that $\mathbf{f}_a \cdot \mathbf{g}_a^\perp = 0$, which violates the non-degeneracy condition (27). This is the desired contradiction, proving that, if $\kappa(s) = 0$ for all $s \in (s_1, s_2)$, then $(\mathbf{e}_a \times \mathbf{e}_b) = 0$. $\square$

5.2. Classification of all local solutions

Locally compatible interfaces with zero curvature or nonzero curvature can now be determined. Recall the notation (23)–(27).

5.2.1. Vertical, horizontal and helical interfaces

Theorem 5.1 (Interfaces with zero curvature). *Assume the hypotheses on the helical groups $G_a \neq G_b$, and assume without loss of generality that $\mathbf{e}_a \cdot \mathbf{e}_b > 0$. Assume that the curvature $\kappa(s) = 0$ on (s_1, s_2). Each locally compatible interface is contained in one of the following cases:*

(i) *(Vertical interfaces).* $\mathbf{e}_a = \mathbf{e}_b$, $\mathbf{t} \cdot \mathbf{f}_a = \mathbf{t} \cdot \mathbf{f}_b = 0$, and $\mathbf{t} \cdot \mathbf{g}_a = \mathbf{t} \cdot \mathbf{g}_b \neq 0$;
(ii) *(Horizontal interfaces).* $\mathbf{e}_a = \mathbf{e}_b$, $\mathbf{t} \cdot \mathbf{f}_a = \mathbf{t} \cdot \mathbf{f}_b \neq 0$, $\mathbf{g}_a \cdot \mathbf{t} = \mathbf{g}_b \cdot \mathbf{t} = 0$, and

$$\mathbf{r}_a = \mathbf{Q}^b_{\mathbf{x}(s_1) \cdot (\mathbf{f}_b - \mathbf{f}_a)} \mathbf{r}_b; \tag{32}$$

(iii) *(Helical interfaces).* *The same as the horizontal interface except that* $\mathbf{g}_a \cdot \mathbf{t} = \mathbf{g}_b \cdot \mathbf{t} \neq 0$.

The interface is given by $\mathbf{x}(s) = (s - s_1)\mathbf{t} + \mathbf{c}$ for some $\mathbf{c} \in \mathbb{R}^2$ and $\mathbf{t} \in \mathbb{S}^1$. In all cases $\mathbf{z}_b$ and $\mathbf{z}_a$ are restricted by matching the formulas (20) at one point on the interface, e.g., $\mathbf{x}(s_1)$.

Proof. Note that (27) implies that $\mathbf{f}_{a,b} \neq 0$. Since $\mathbf{t}(s) = \mathbf{t} = const$, we have $\mathbf{e}_a \times \mathbf{e}_b \neq 0$ by Lemma 5.1 and so $\mathbf{e}_a = \mathbf{e}_b = \mathbf{e}$. Thus, $\mathbf{Q}^a_{(\cdot)} = \mathbf{Q}^b_{(\cdot)} = \mathbf{Q}_{(\cdot)}$ and $\mathbf{W}^a = \mathbf{W}^b = \mathbf{W}$. Hence, by explicitly differentiating the compatibility Eq. (28) and pre-multiplying this equation by $\mathbf{Q}_{-\mathbf{x}(s) \cdot \mathbf{f}_a}$, we obtain a condition equivalent to local compatibility in this case:

$$(\mathbf{t} \cdot \mathbf{f}_b) \mathbf{Q}_{\mathbf{x}(s) \cdot (\mathbf{f}_b - \mathbf{f}_a)} \mathbf{W} \mathbf{r}_b - (\mathbf{t} \cdot \mathbf{f}_a) \mathbf{W} \mathbf{r}_a = (\mathbf{g}_a \cdot \mathbf{t} - \mathbf{g}_b \cdot \mathbf{t}) \mathbf{e} \tag{33}$$

---

[7] If they are linearly independent at a single point, then, by continuity, they must be linearly independent on some interval.

for $s \in (s_1, s_2)$. Here, $\mathbf{Wr}_a$ and $\mathbf{Q}_{\mathbf{x}(s)\cdot(\mathbf{f}_b-\mathbf{f}_a)}\mathbf{Wr}_b$ are both perpendicular to $\mathbf{e}$. Thus, by dotting this quantity with $\mathbf{e}$, we see that $\mathbf{g}_a \cdot \mathbf{t}$ must equal $\mathbf{g}_b \cdot \mathbf{t}$. This condition is necessary in all cases as stated in the theorem.

Substituting this back into (33), the right-hand side vanishes. Then, by differentiating this equation, we obtain the necessary condition

$$(\mathbf{t} \cdot \mathbf{f}_b)(\mathbf{t} \cdot (\mathbf{f}_b - \mathbf{f}_a))\mathbf{Q}_{\mathbf{x}(s)\cdot(\mathbf{f}_b-\mathbf{f}_a)}\mathbf{r}_b = 0 \tag{34}$$

for $s \in (s_1, s_2)$. By assumption $\mathbf{r}_b$ cannot be zero, so $\mathbf{Q}_{\mathbf{x}(s)\cdot(\mathbf{f}_b-\mathbf{f}_a)}\mathbf{r}_b$ is not zero. Thus, there are only two possibilities for local compatibility in this case:

(a) Either, $\mathbf{t} \cdot \mathbf{f}_b = 0$;
(b) Or, $\mathbf{t} \cdot \mathbf{f}_b \neq 0$ and $\mathbf{t} \cdot (\mathbf{f}_b - \mathbf{f}_a) = 0$.

We suppose (a). Then, in substituting $\mathbf{t} \cdot \mathbf{f}_b = 0$ back into the first in (33), we have a locally compatible helical structure if and only if $(\mathbf{t} \cdot \mathbf{f}_a)\mathbf{Wr}_a = 0$; that is, if and only if $\mathbf{t} \cdot \mathbf{f}_a = 0$. In combining all the identities, we obtain Case (i) in the theorem. The inequality $\mathbf{g}_{a,b} \cdot \mathbf{t} \neq 0$ follows from the nondegeneracy conditions (27) assumed on the group parameters. Thus, hypothesis (a) gives Case (i) of the theorem.

Now, we suppose (b) above. Note that since $\mathbf{x}'(s) = \mathbf{t} = const.$, the curve is given by $\mathbf{x}(s) = (s - s_1)\mathbf{t} + \mathbf{c}$ for some $\mathbf{c} \in \mathbb{R}^2$ (as stated in the theorem). Making use of this fact, we observe that $\mathbf{Q}_{\mathbf{x}(s)\cdot(\mathbf{f}_b-\mathbf{f}_a)} = \mathbf{Q}_{\mathbf{c}\cdot(\mathbf{f}_b-\mathbf{f}_a)} = const.$ since $\mathbf{t} \cdot (\mathbf{f}_b - \mathbf{f}_a) = 0$. Substituting this into (33), we have a locally compatible interface if and only if

$$(\mathbf{t} \cdot \mathbf{f}_b)\mathbf{Q}_{\mathbf{c}\cdot(\mathbf{f}_b-\mathbf{f}_a)}\mathbf{Wr}_b = (\mathbf{t} \cdot \mathbf{f}_a)\mathbf{Wr}_a. \tag{35}$$

Noting that $\mathbf{Q}_{(\cdot)}$ and $\mathbf{W}$ commute, we can remove $\mathbf{W}$ from (35), and we can cancel the nonzero terms $\mathbf{t} \cdot \mathbf{f}_b = \mathbf{t} \cdot \mathbf{f}_a$. Thus, we have necessarily that $|\mathbf{r}_b| = |\mathbf{r}_a|$ and $\mathbf{Q}_{\mathbf{x}(s_1)\cdot(\mathbf{f}_b-\mathbf{f}_a)}\mathbf{r}_b = \mathbf{r}_a$. This condition is also sufficient for (35). Therefore, necessary and sufficient conditions for local compatibility under hypotheses (b) are given in Cases (ii) and (iii) of the theorem. □

5.2.2. Elliptic interfaces

Theorem 5.2 (Interfaces with nonzero curvature)**.** *Assume the hypotheses on the helical groups $G_a \neq G_b$, assume the hypothesis on the interface, and assume that the curvature $\kappa(s) \neq 0$ on (s_1, s_2). Introduce an orthonormal basis $\mathbf{e}_1 = \mathbf{e}_b \times \mathbf{e}_a/|\mathbf{e}_b \times \mathbf{e}_a|$, $\mathbf{e}_2 = (\mathbf{e}_b - \mathbf{e}_a)/|\mathbf{e}_b - \mathbf{e}_a|$ and $\mathbf{e}_3 = \mathbf{e}_1 \times \mathbf{e}_2$. Define $0 \leq \theta_{a,b} < 2\pi$ and $\rho_{a,b} > 0$ by $\rho_a \mathbf{Q}^a_{\theta_a}\mathbf{e}_1 = \mathbf{r}_a$ and $\rho_b \mathbf{Q}^b_{\theta_b}\mathbf{e}_1 = \mathbf{r}_b$. Note that $\mathbf{e}_a = -\sin\xi\,\mathbf{e}_2 + \cos\xi\,\mathbf{e}_3$, $\mathbf{e}_b = \sin\xi\,\mathbf{e}_2 + \cos\xi\,\mathbf{e}_3$ for a suitable $0 < \xi < \pi$, $\xi \neq \pi/2$. Each locally compatible interface is contained in one of the following cases:*

(i) *(Type 1 Elliptic interfaces). $\mathbf{f}_a = \mathbf{f}_b$, $\mathbf{g}_a = -\mathbf{g}_b$, $\rho_a = \rho_b$, $\theta_a = \theta_b$. In non-arclength parameterization the interface is given by*

$$\tilde{\mathbf{x}}(t) = t\mathbf{u} + (\rho_a \tan\xi \sin(t + \theta_a) + c)\mathbf{v}, \tag{36}$$

  where $\mathbf{u} \cdot \mathbf{g}_b = \mathbf{v} \cdot \mathbf{f}_b = 0$, $\mathbf{u} \cdot \mathbf{f}_b = \mathbf{v} \cdot \mathbf{g}_b = 1$, $c \in \mathbb{R}$ and $t \in (t_1, t_2)$ for the interval chosen below.
(ii) *(Type 2 Elliptic interfaces). $\mathbf{f}_a = -\mathbf{f}_b$, $\mathbf{g}_a = \mathbf{g}_b$, $\rho_a = \rho_b$, $\theta_a = -\theta_b$. In non-arclength parameterization the interface is given by*

$$\tilde{\mathbf{x}}(t) = t\mathbf{u} + (\rho_a \cot\xi \sin(-t + \theta_a) + c)\mathbf{v} \tag{37}$$

  with $\mathbf{u}$, $\mathbf{v}$, c as above and $t \in (t_1, t_2)$ for the interval below.

The formulas for the interface can be converted to arclength parameterization by the standard method of writing $\mathbf{x}(s) = \tilde{\mathbf{x}}(t(s))$ where $t(s)$ is the inverse of $s(t) = \int_{t_1}^{t} |\tilde{\mathbf{x}}'(\tilde{t})|d\tilde{t} + s_1$ and t_2 is such that $s(t_2) = s_2$.

Proof. The introduction of the basis $(\mathbf{e}_1, \mathbf{e}_2, \mathbf{e}_3)$ and ξ are justified by $\mathbf{e}_a \times \mathbf{e}_b \neq 0$ (see Lemma 5.1) and $\mathbf{e}_1 \cdot \mathbf{e}_{a,b} = 0$. Consider the integrated form of (28),

$$\mathbf{Q}^a_{\mathbf{x}(s)\cdot\mathbf{f}_a+\theta_a}(\rho_a\mathbf{e}_1 + (\mathbf{x}(s) \cdot \mathbf{g}_a)\mathbf{e}_a) = \mathbf{Q}^b_{\mathbf{x}(s)\cdot\mathbf{f}_b+\theta_b}(\rho_b\mathbf{e}_1 + (\mathbf{x}(s) \cdot \mathbf{g}_b)\mathbf{e}_b) + \mathbf{c}. \tag{38}$$

The proof consists of identifying certain components of (38). Dotting (38) by $\mathbf{e}_1$, $\mathbf{e}_2$ and $\mathbf{e}_3$, respectively, yields the equations

$$\rho_a \cos(\mathbf{x}(s) \cdot \mathbf{f}_a + \theta_a) = \rho_b \cos(\mathbf{x}(s) \cdot \mathbf{f}_b + \theta_b) + c_1,$$
$$\rho_a \sin(\mathbf{x}(s) \cdot \mathbf{f}_a + \theta_a) - \tan\xi\,(\mathbf{x}(s) \cdot \mathbf{g}_a) = \rho_b \sin(\mathbf{x}(s) \cdot \mathbf{f}_b + \theta_b) + \tan\xi\,(\mathbf{x}(s) \cdot \mathbf{g}_b) + c_2/\cos\xi,$$
$$\rho_a \sin(\mathbf{x}(s) \cdot \mathbf{f}_a + \theta_a) + \cot\xi\,(\mathbf{x}(s) \cdot \mathbf{g}_a) = -\rho_b \sin(\mathbf{x}(s) \cdot \mathbf{f}_b + \theta_b) + \cot\xi\,(\mathbf{x}(s) \cdot \mathbf{g}_b) + c_3/\sin\xi. \tag{39}$$

We first show that the nonzero vectors $\mathbf{f}_a$ and $\mathbf{f}_b$ are parallel. Suppose, for the sake of a contradiction, they are not. Then they are linearly independent, and so there exist linearly independent reciprocal vectors $\mathbf{f}^a$, $\mathbf{f}^b$ satisfying $\mathbf{f}_a \cdot \mathbf{f}^a = 1, \mathbf{f}_b \cdot \mathbf{f}^b = 1, \mathbf{f}_a \cdot \mathbf{f}^b = \mathbf{f}_b \cdot \mathbf{f}^a = 0$. Therefore, we express the tangent to the interface in the reciprocal basis:

$$\mathbf{t}(s) = \eta_a(s)\mathbf{f}^a + \eta_b(s)\mathbf{f}^b, \tag{40}$$

where the parameters $\eta_{a,b}(s)$ are continuously differentiable due to the hypothesis on the interface. We differentiate (39)$_2$ and (39)$_3$ with respect to s, eliminate $\cos(\mathbf{x}(s) \cdot \mathbf{f}_a + \theta_a)$ in both cases using (39)$_1$, and add and subtract the resulting equations. This gives

$$(2\rho_b \cos(\mathbf{x}(s) \cdot \mathbf{f}_b + \theta_b)\mathbf{f}_a + \mathbf{k}_1) \cdot \mathbf{t}(s) = 0, \quad (2\rho_b \cos(\mathbf{x}(s) \cdot \mathbf{f}_b + \theta_b)\mathbf{f}_b + \mathbf{k}_2) \cdot \mathbf{t}(s) = 0, \tag{41}$$

where $\mathbf{k}_1$ and $\mathbf{k}_2$ are explicit functions of ξ, c_1, $\mathbf{f}_a$, $\mathbf{g}_a$, $\mathbf{g}_b$. To further simplify, we insert (40) into (41), multiply (41)$_1$ by $\eta_b(s)$ and (41)$_2$ by $\eta_a(s)$, and add to get

$$\eta_a(s)^2(\mathbf{k}_2 \cdot \mathbf{f}^a) + \eta_a(s)\eta_b(s)(\mathbf{k}_1 \cdot \mathbf{f}^a + \mathbf{k}_2 \cdot \mathbf{f}^b) + \eta_b(s)^2(\mathbf{k}_1 \cdot \mathbf{f}^b) = 0. \tag{42}$$

Since the curvature $\kappa(s)$ is non-zero, there exists an $(\tilde{s}_1, \tilde{s}_2) \subset (s_1, s_2)$ such that $\eta_a(s)$ and $\eta_a'(s) \neq 0$ on this sub-interval. We divide through by $\eta_a(s)^2 \neq 0$ in (42) to obtain a quadratic equation in $\lambda(s) = \eta_b(s)/\eta_a(s)$ on this reduced interval. If $\lambda'(s) \neq 0$ on $(\tilde{s}_1, \tilde{s}_2)$, then it immediately follows that the coefficients of this quadratic equation must vanish, i.e.,

$$\mathbf{k}_1 \cdot \mathbf{f}^b = \mathbf{k}_2 \cdot \mathbf{f}^a = \mathbf{k}_1 \cdot \mathbf{f}^a + \mathbf{k}_2 \cdot \mathbf{f}^b = 0. \tag{43}$$

The derivative is indeed non-vanishing: We notice that $\mathbf{t}(s)/\eta_a(s) = \mathbf{f}^a + \lambda(s)\mathbf{f}^b$ by definition, and consequently, differentiating this quantity yields the desired result since both $\kappa(s)$ and $\eta_a'(s)$ are non-vanishing on this interval. Hence, (43) is a necessary condition on the parameters. These equations are then solved by expressing $\mathbf{k}_1$, $\mathbf{k}_2$ in the basis $\mathbf{f}_a$, $\mathbf{f}_b$, yielding

$$\mathbf{k}_1 = \delta\mathbf{f}_a, \quad \mathbf{k}_2 = -\delta\mathbf{f}_b, \quad \text{for some } \delta \in \mathbb{R}. \tag{44}$$

We insert (44) into (41) to obtain

$$(2\rho_b \cos(\mathbf{x}(s) \cdot \mathbf{f}_b + \theta_b) + \delta)\eta_a(s) = 0, \quad (-2\rho_b \cos(\mathbf{x}(s) \cdot \mathbf{f}_b + \theta_b) - \delta)\eta_b(s) = 0. \tag{45}$$

Since $\eta_a(s) \neq 0$ on $(\tilde{s}_1, \tilde{s}_2)$, we observe that $\cos(\mathbf{x}(s) \cdot \mathbf{f}_b + \theta_b) = const$ on this interval. By the smoothness hypothesis of the interface, it follows that $\mathbf{x}(s) \cdot \mathbf{f}_b = const$ on this interval. By differentiation and the parameterization for $\mathbf{t}(s)$ in (40), we conclude $\eta_b(s) = 0$ on this interval. But this means that $\eta_a(s) = 1/|\mathbf{f}^a|$ on this interval since the tangent is a unit vector. This contradicts the fact that $\eta_a'(s) \neq 0$ on $(\tilde{s}_1, \tilde{s}_2)$. Therefore, $\mathbf{f}_a$ and $\mathbf{f}_b$ are in fact parallel.

Let $\mathbf{f}_b = \lambda\mathbf{f}_a$ for some $\lambda \neq 0$ (recall (27)). We show that $\lambda = \pm 1$. We work in a sufficiently small neighborhood of $s^* \in (s_1, s_2)$ where $\mathbf{t}(s^*) \cdot \mathbf{f}_a \neq 0$. Under our smoothness assumptions we can differentiate (39)$_1$ as many times as we like near s^* as long as we cancel the $\mathbf{t}(s) \cdot \mathbf{f}_a$ after each differentiation. Comparing the first and third derivative of (39)$_1$ we get that $\lambda^2 = 1$, so $\mathbf{f}_b = \pm\mathbf{f}_a$. We treat these two cases separately.

Suppose $\mathbf{f}_b = \mathbf{f}_a$. Again we work near $s = s^*$. Comparing the first and second derivative of (39)$_1$, we get that $\rho_a(\cos(\mathbf{x}(s) \cdot \mathbf{f}_a + \theta_a), \sin(\mathbf{x}(s) \cdot \mathbf{f}_a + \theta_a)) = \rho_b(\cos(\mathbf{x}(s) \cdot \mathbf{f}_a + \theta_b), \sin(\mathbf{x}(s) \cdot \mathbf{f}_a + \theta_b))$. Since $\rho_{a,b} > 0$ and $0 \leq \theta_{a,b} < 2\pi$, this shows that $\rho_a = \rho_b$ and $\theta_a = \theta_b$. The derivative of (39)$_2$ with respect to s near s^* implies immediately that $\mathbf{g}_a = -\mathbf{g}_b$. At this point (39)$_{1,2}$ are satisfied with $c_1 = c_2 = 0$ and (39)$_3$ becomes a condition that determines $\mathbf{x}(s)$. Consider an arbitrary regular parameterization $\tilde{\mathbf{x}} : (t_1, t_2) \to \mathbb{R}^2$ given by $\tilde{\mathbf{x}}(t) = \zeta_1(t)\mathbf{u} + \zeta_2(t)\mathbf{v}$, where $(\mathbf{u}, \mathbf{v})$ are reciprocal vectors to the linearly independent vectors $\mathbf{f}_b$, $\mathbf{g}_b$ as defined by $\mathbf{u} \cdot \mathbf{g}_b = \mathbf{v} \cdot \mathbf{f}_b = 0, \mathbf{u} \cdot \mathbf{f}_b = \mathbf{v} \cdot \mathbf{g}_b = 1$. We substitute $\mathbf{x}(s(t)) = \tilde{\mathbf{x}}(t)$ into (39)$_3$ (for $s(t) = \int_{t_1}^t |\tilde{\mathbf{x}}'(\tilde{t})| d\tilde{t} + s_1$ with t_2 such that $s(t_2) = s_2$) to derive the necessary and sufficient conditions on the arc-length parameterized curve $\mathbf{x} : (s_1, s_2) \to \mathbb{R}^2$. We find $\zeta_2(t) = \rho_b \tan\xi \sin(\zeta_1(t) + \theta_b) + c$ for any $c \in \mathbb{R}$ solves (39)$_3$. This shows that the interface is the graph of a function in the direction $\mathbf{f}_b$, and so without loss of generality, we can set $\zeta_1(t) = t$ and parameterize by arclength to obtain a generic expression for the interface curve $\mathbf{x}(s)$ satisfying (39)$_3$. This is given by (36) in the theorem.

Suppose on the other hand $\mathbf{f}_b = -\mathbf{f}_a$. Again comparing the first and second derivative of (39)$_1$, we now get that $\rho_a = \rho_b$ and $\theta_a = -\theta_b$. In this case the derivative of (39)$_3$ with respect to s near s^* implies that $\mathbf{g}_a = \mathbf{g}_b$, and (39)$_2$ gives the formula (37) for the interface. $\square$

Examples of vertical, horizontal, helical and elliptic interfaces consistent with Theorems 5.1 and 5.2 are given in Fig. 3. All four types of interface can be extended to be global solutions in typical cases. By substituting the formulas for the interface given in Theorem 5.2.2 into the formula (20), one can prove that the elliptic interfaces are indeed ellipses in the helical configuration. Elliptic interfaces are typically not orientable in the sense of (22): this explains the appearance of the overlapping reference domains in Fig. 3(d), which have been displaced from each other to be easily visible. Fig. 3(d) illustrates motion of the elliptical interface, but typically vertical and helical interfaces cannot be moved. We discuss further the mobility of interfaces in Section 8.

6. Local compatibility using near neighbor generators

Nearest neighbor generators provide convenient descriptors for a helical structure, as neighbors in the $\mathbb{Z}^2$ lattice are neighboring points in the helical structure. These generators have other key properties as shown Section 3: (i) they can be explicitly obtained for any discrete Abelian helical group under mild assumptions, and (ii) they have a suitable reference configuration. By examining analogs in helical structures of the concepts of slip and twinning in crystals, we have noticed that the study of compatibility using a fixed set of nearest neighbor generators for each phase is too restrictive: some of the excluded cases are interesting. These cases include examples of additional compatible interfaces (analogs of twins) obtained by switching to a different choice of nearest neighbor generators for one of the phases. Therefore, in this section we are led
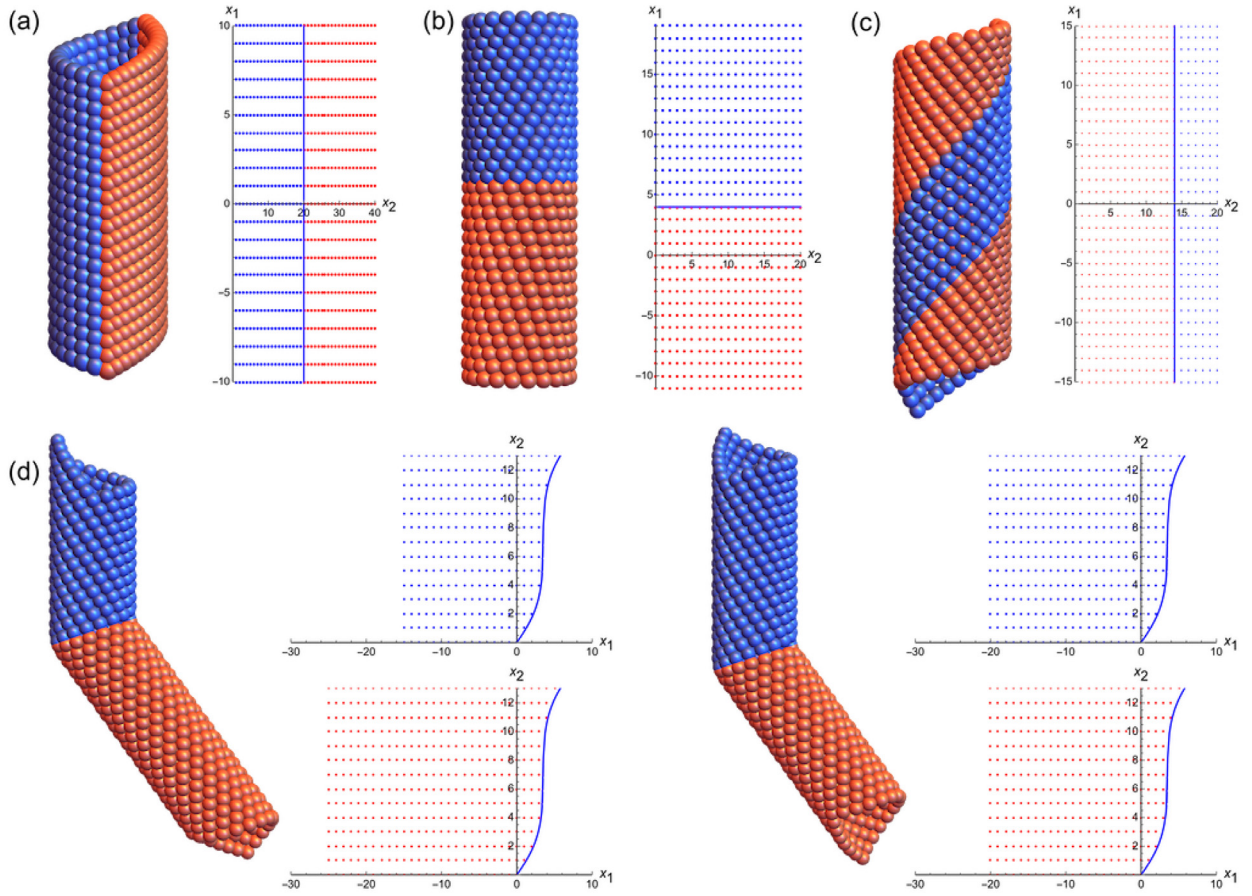
Fig. 3. Examples of vertical, horizontal, helical, and elliptical interfaces ((a)–(d)) between phase a (blue) and phase b (red) shown in the deformed configuration (left) and reference domain (right; interfaces in blue). The local solutions are extended to global loops, where possible. They correspond to the choices $|\mathbf{r}_a| = |\mathbf{r}_b| = 1$ (all cases) and (a) $\mathbf{x}(s) = (s, 20)$, $\mathbf{f}_a = (0, 0.25)$, $\mathbf{f}_b = (0, 0.15)$, $\mathbf{g}_a = (0.28, -0.08)$, $\mathbf{g}_b = (0.28, 0.084)$ (b) $\mathbf{x}(s) = (4, s)$, $\mathbf{f}_a = (0.12, \pi/10)$, $\mathbf{f}_b = (-0.4, \pi/10)$, $\mathbf{g}_a = (0.262, 0)$, $\mathbf{g}_b = (0.3, 0)$, (c) $\mathbf{x}(s) = (s, 14)$, $\mathbf{f}_a = (0.2, 0.22)$, $\mathbf{f}_b = (0.2, 0.33)$, $\mathbf{g}_a = (0.27, -0.18)$, $\mathbf{g}_b = (0.27, 0.081)$, (d) $\tilde{\mathbf{x}}(t) = t(3.5/\pi, 7/\pi) + \tan(\pi/10)\sin(t)(10/3, -5/3)$ (non-arclength parameterization, see Theorem 5.2), $\mathbf{f}_a = \mathbf{f}_b = (2\pi/35, 4\pi/35)$, $\mathbf{g}_a = -\mathbf{g}_b = (-0.24, 0.12)$. (For interpretation of the references to color in this figure legend, the reader is referred to the web version of this article.)

to consider a certain precise notion of *near neighbor generators* with the properties (i) and (ii), and to study the resulting compatible interfaces. The concept of compatibility used here with near neighbor generators is the same as the one used above.

6.1. Lattice invariant transformations

We first recall the basic invariance of the $\mathbb{Z}^2$ lattice (Pitteri and Zanzotto, 2002). The set of invertible linear transformations mapping $\mathbb{Z}^2$ to $\mathbb{Z}^2$ is

$$GL(\mathbb{Z}^2) = \left\{ \boldsymbol{\mu} \in \mathbb{R}^{2 \times 2} : \mu_{ij} \in \mathbb{Z}, \ i = 1, 2, \ j = 1, 2, \ \det \boldsymbol{\mu} \in \{\pm 1\} \right\}. \tag{46}$$

Consider the nearest neighbor parameterizations of the two helical phases given by (20), and bring out the dependence of these formulas on the group parameters by writing these positions as $\mathbf{y}_a(p, q) = \mathbf{y}(p, q; \mathbf{f}_a, \mathbf{g}_a, \mathbf{r}_a, \mathbf{z}_a)$ and $\mathbf{y}_b(p, q) = \mathbf{y}(p, q; \mathbf{f}_b, \mathbf{g}_b, \mathbf{r}_b, \mathbf{z}_b)$. Each element $\boldsymbol{\mu} \in GL(\mathbb{Z}^2)$ gives an alternative parameterization of these same two given helical phases by replacing $(p, q) = \boldsymbol{\mu}(\tilde{p}, \tilde{q})$, with $(\tilde{p}, \tilde{q})$ in the domains $\tilde{\mathcal{D}}_{a,b} = \boldsymbol{\mu}^{-1}(\mathbb{Z} \times \{1, \ldots, q^\star_{a,b}\})$, respectively. As can be seen from the formulas (20), the matrix $\boldsymbol{\mu}$ can be moved onto the group parameters. The positions

$$\mathbf{y}(\tilde{p}, \tilde{q}; \boldsymbol{\mu}^T \mathbf{f}_a, \boldsymbol{\mu}^T \mathbf{g}_a, \mathbf{r}_a, \mathbf{z}_a), \quad (\tilde{p}, \tilde{q}) \in \tilde{\mathcal{D}}_a, \quad \mathbf{y}(\tilde{p}, \tilde{q}; \boldsymbol{\mu}^T \mathbf{f}_b, \boldsymbol{\mu}^T \mathbf{g}_b, \mathbf{r}_b, \mathbf{z}_b), \quad (\tilde{p}, \tilde{q}) \in \tilde{\mathcal{D}}_b, \tag{47}$$

are therefore the same two sets of atomic positions as given by $\mathbf{y}_a(p, q)$, $\mathbf{y}_b(p, q)$. If the two phases are compatible across an interface $(p(s), q(s))$, then the positions (47) are compatible across the interface $(\tilde{p}(s), \tilde{q}(s)) = \boldsymbol{\mu}^{-1}(p(s), q(s))$.

As can be seen from Section 3, nearest neighbor generators are defined using a particular helical structure, i.e., a particular choice of $(\mathbf{f}, \mathbf{g})$. Thus, it may happen that the formulas for nearest neighbor generators (given just after (59)) evaluated at

the new group parameters ($\boldsymbol{\mu}^T\mathbf{f}$, $\boldsymbol{\mu}^T\mathbf{g}$) are not nearest neighbor generators. Also, it can happen that formulas for non-nearest neighbor generators evaluated at particular choices of $\mathbf{f}$ and $\mathbf{g}$ give nearest neighbor generators when evaluated at ($\boldsymbol{\mu}^T\mathbf{f}$, $\boldsymbol{\mu}^T\mathbf{g}$).

In summary, given certain formulas for generators g_1, g_2 of the group G evaluated at ($\mathbf{f}$, $\mathbf{g}$), then those formulas evaluated at ($\boldsymbol{\mu}^T\mathbf{f}$, $\boldsymbol{\mu}^T\mathbf{g}$) give exactly the same helical structure. However, if g_1, g_2 evaluated at ($\mathbf{f}$, $\mathbf{g}$) are nearest neighbor generators, then g_1, g_2 evaluated at ($\boldsymbol{\mu}^T\mathbf{f}$, $\boldsymbol{\mu}^T\mathbf{g}$) are not generally nearest neighbor generators, and vice versa. If the *same* $\boldsymbol{\mu} \in GL(\mathbb{Z}^2)$ is applied to compatible phases a and b, then they remain compatible, the interface is unchanged in the helical configuration, but the description of the interface in terms of g_1, g_2 evaluated at ($\boldsymbol{\mu}^T\mathbf{f}$, $\boldsymbol{\mu}^T\mathbf{g}$) changes to ($\tilde{p}(s), \tilde{q}(s)$) = $\boldsymbol{\mu}^{-1}(p(s), q(s))$.

We can also transform group parameters using *different* elements of $GL(\mathbb{Z}^2)$ for the two lattices. By the discussion above, we can without loss of generality leave one lattice unchanged, since applying a $\boldsymbol{\mu} \in GL(\mathbb{Z}^2)$ to both sets of generators is a equivalent to a change of reference configuration. Let us fix the nearest neighbor generators of phase a so that the group parameter are ($\mathbf{f}_a$, $\mathbf{g}_a$) and apply $\boldsymbol{\mu} \in GL(\mathbb{Z}^2)$ to the nearest neighbor generators of phase b so that the group parameters are ($\boldsymbol{\mu}^T\mathbf{f}_b$, $\boldsymbol{\mu}^T\mathbf{g}_b$). Again, if we use the appropriate domains of integers, both structures are exactly the same. However, the meaning of the compatibility conditions changes, because nearby pairs of integers do not in general give nearby points in the helical structure of phase b.

This is not a problem—when thinking in terms of phase transformations—as long as nearby points on the helical structure prior to transformation remain *reasonably close* after transformation. If we ignore the fact that $\boldsymbol{\mu} \in GL(\mathbb{Z}^2)$ and think of $\boldsymbol{\mu}$ as a general 2×2 matrix, the formulas for generators depend smoothly on $\boldsymbol{\mu}$. Thus, a simple measure of "reasonable closeness" is $|\boldsymbol{\mu} - \mathbf{I}|$.

With these physical considerations in mind, we can generalize the local compatibility condition, Theorem 5.1, for vertical, horizontal and helical interfaces to include other choices of generators beyond those for nearest neighbor generators $\{\mathbf{f}_a, \mathbf{g}_a\}$ and $\{\mathbf{f}_b, \mathbf{g}_b\}$. Referring to Theorem 5.1, the condition is

$$\left((\mathbf{f}_b, \mathbf{g}_b)^T \boldsymbol{\mu} - (\mathbf{f}_a, \mathbf{g}_a)^T\right)\mathbf{t} = 0 \tag{48}$$

from some unit tangent $\mathbf{t}$ and appropriate inequalities that define the subcases vertical, horizontal and helical. (We have simply replaced $\{\mathbf{f}_b, \mathbf{g}_b\}$ in Theorem 5.1 with $\{\boldsymbol{\mu}^T\mathbf{f}_b, \boldsymbol{\mu}^T\mathbf{g}_b\}$.) Note that the nondegeneracy condition (27) is satisfied for $\{\boldsymbol{\mu}^T\mathbf{f}_b, \boldsymbol{\mu}^T\mathbf{g}_b\}$ if and only if it is satisfied for $\{\mathbf{f}_b, \mathbf{g}_b\}$.

We focus on vertical, horizontal and helical interfaces here, because no additional locally compatible elliptic interfaces are obtained if we include a lattice invariant transformation $\boldsymbol{\mu} \in GL(\mathbb{Z}^2)$ of phase b. Also, as discussed at the beginning of Section 5, recall that opposite sides of the reference interface need not be mapped to opposite sides of the deformed interface.

Following the remark above about "near closeness" we define *near neighbor generators* as those associated to $\boldsymbol{\mu} \in GL(\mathbb{Z}^2)$ of the form

$$\mathcal{N}(GL(\mathbb{Z}^2)) = \left\{ \begin{pmatrix} \sigma_1 & \sigma_2 \\ \sigma_3 & \sigma_4 \end{pmatrix} : \sigma_{1,2,3,4} \in \{\pm 1, 0\}, \ \sigma_1\sigma_4 - \sigma_2\sigma_3 \in \{\pm 1\} \right\}. \tag{49}$$

When the two phases a and b are the same these represent slip by one lattice spacing, or twinning. An easy enumeration shows that

$$\mathcal{N}(GL(\mathbb{Z}^2)) = \mathcal{N}^{(+)}(GL(\mathbb{Z}^2)) \cup \mathcal{N}^{(-)}(GL(\mathbb{Z}^2)), \tag{50}$$

where

$$\mathcal{N}^{(+)}(GL(\mathbb{Z}^2)) = \left\{ \pm\begin{pmatrix} 1 & 0 \\ 0 & 1 \end{pmatrix}, \pm\begin{pmatrix} 0 & -1 \\ 1 & 0 \end{pmatrix}, \pm\begin{pmatrix} 1 & -1 \\ 1 & 0 \end{pmatrix}, \pm\begin{pmatrix} 1 & 0 \\ -1 & 1 \end{pmatrix}, \pm\begin{pmatrix} 0 & 1 \\ -1 & 1 \end{pmatrix}, \right.$$
$$\left. \pm\begin{pmatrix} 1 & 1 \\ -1 & 0 \end{pmatrix}, \pm\begin{pmatrix} 1 & -1 \\ 0 & 1 \end{pmatrix}, \pm\begin{pmatrix} 1 & 1 \\ 0 & 1 \end{pmatrix}, \pm\begin{pmatrix} 1 & 0 \\ 1 & 1 \end{pmatrix}, \pm\begin{pmatrix} 0 & -1 \\ 1 & 1 \end{pmatrix} \right\}; \tag{51}$$
$$\mathcal{N}^{(-)}(GL(\mathbb{Z}^2)) = \begin{pmatrix} 0 & 1 \\ 1 & 0 \end{pmatrix} \mathcal{N}^{(+)}(GL(\mathbb{Z}^2)),$$

and the superscript ($\pm$) indicates the sign of the determinant.

7. Slip and twinning in helical structures

In this section, we consider the two phases a and b to be the same, in the sense that they are related by an orthogonal transformation and translation. In this case, compatible deformations are analogous to slip or twinning. Our main question is whether we can have compatible vertical, horizontal or helical interfaces, between two copies of the same phase that are oriented differently.

7.1. Local compatibility of helical structures in the same phase

We define precisely what it means that phase b is the same phase as phase a. Let phase a be given with nearest neighbor group parameterization $\{\mathbf{f}, \mathbf{g}\}$, where we drop the subscript "a" for simplicity. The positions of phase a are $\mathbf{y}(p, q; \mathbf{f}, \mathbf{g}, \mathbf{r}, \mathbf{z})$, where $(p, q) \in \mathcal{D} = \mathbb{Z} \times \{1, \ldots, q^\star\}$. In view of Theorem 5.1, we have extended the definition of $\mathbf{y}$ to $\mathbf{x} = (p, q) \in \mathcal{D}^c = \mathbb{R} \times (0, q^\star)$.

Guided by the basic invariance of quantum mechanics—orthogonal transformations with determinant ± 1 and translations—we consider a second copy of phase a given by

$$\hat{\mathbf{Q}}\mathbf{y}(\mathbf{x}; \boldsymbol{\mu}^T\mathbf{f}, \boldsymbol{\mu}^T\mathbf{g}, \mathbf{r}, \mathbf{z}) + \hat{\mathbf{c}}, \quad \hat{\mathbf{Q}} \in O(3), \quad \hat{\mathbf{c}} \in \mathbb{R}^3, \quad \mathbf{x} = (p, q) \in \boldsymbol{\mu}^{-1}\mathcal{D}^c, \tag{52}$$

where we have allowed for a change to near neighbor generators by introducing $\boldsymbol{\mu} \in \mathcal{N}^{(\sigma)}(GL(\mathbb{Z}^2))$.

We seek a locally compatible vertical, horizontal and helical interfaces between $\mathbf{y}(\mathbf{x}; \mathbf{f}, \mathbf{g}, \mathbf{r}, \mathbf{z})$ and the copy $\hat{\mathbf{Q}}\mathbf{y}(\mathbf{x}; \boldsymbol{\mu}^T\mathbf{f}, \boldsymbol{\mu}^T\mathbf{g}, \mathbf{r}, \mathbf{z}) + \hat{\mathbf{c}}$ at an interface $\mathbf{x}(s) \in \mathcal{D}^c \cap \boldsymbol{\mu}^{-1}\mathcal{D}^c$ for $s \in (s_1, s_2)$. In these cases, the two phases have a common axis, so that necessarily $\hat{\mathbf{Q}}\mathbf{e} = \pm\mathbf{e}$. The four families of $\hat{\mathbf{Q}} \in O(3)$ satisfying $\hat{\mathbf{Q}}\mathbf{e} = \pm\mathbf{e}$ are

$$\det\hat{\mathbf{Q}} = +1 \implies \begin{cases} \hat{\mathbf{Q}} = -\mathbf{I} + 2\mathbf{e}^\perp \otimes \mathbf{e}^\perp, \quad \mathbf{e}^\perp \cdot \mathbf{e} = 0, \quad |\mathbf{e}^\perp| = 1, \quad \hat{\mathbf{Q}}\mathbf{Q} = \mathbf{Q}^T\hat{\mathbf{Q}}, \text{ or} \\ \hat{\mathbf{Q}} = \mathbf{R_e}, \quad \mathbf{R_e}\mathbf{e} = \mathbf{e}, \quad \mathbf{R_e} \in SO(3), \quad \hat{\mathbf{Q}}\mathbf{Q} = \mathbf{Q}\hat{\mathbf{Q}}, \end{cases}$$

$$\det\hat{\mathbf{Q}} = -1 \implies \begin{cases} \hat{\mathbf{Q}} = \mathbf{I} - 2\mathbf{e}^\perp \otimes \mathbf{e}^\perp, \quad \mathbf{e}^\perp \cdot \mathbf{e} = 0, \quad |\mathbf{e}^\perp| = 1, \quad \hat{\mathbf{Q}}\mathbf{Q} = \mathbf{Q}^T\hat{\mathbf{Q}}, \text{ or} \\ \hat{\mathbf{Q}} = -\mathbf{R_e}, \quad \mathbf{R_e}\mathbf{e} = \mathbf{e}, \quad \mathbf{R_e} \in SO(3), \quad \hat{\mathbf{Q}}\mathbf{Q} = \mathbf{Q}\hat{\mathbf{Q}}. \end{cases} \tag{53}$$

The second copy of phase a can then be expressed in the form

$$\hat{\mathbf{Q}}\mathbf{y}(\mathbf{x}; \boldsymbol{\mu}^T\mathbf{f}, \boldsymbol{\mu}^T\mathbf{g}, \mathbf{r}, \mathbf{z}) + \hat{\mathbf{c}} = \mathbf{y}(\mathbf{x}; \pm\boldsymbol{\mu}^T\mathbf{f}, (\pm)\boldsymbol{\mu}^T\mathbf{g}, \hat{\mathbf{Q}}\mathbf{r}, \hat{\mathbf{Q}}\mathbf{z} + \hat{\mathbf{c}}), \quad \mathbf{x} \in \boldsymbol{\mu}^{-1}\mathcal{D}^c. \tag{54}$$

Here, the $\pm$ arises because $\hat{\mathbf{Q}}\mathbf{Q}_\theta = \mathbf{Q}_{\pm\theta}\hat{\mathbf{Q}}$ for some choice of $\pm$ in all cases of (53); the other (independent) choice $(\pm)$ arises from $\hat{\mathbf{Q}}\mathbf{e} = (\pm)\mathbf{e}$. We identify phase b with the copy of phase a described in (54) and characterize solutions to the compatibility conditions (48) corresponding to vertical, horizontal and helical interfaces for near neighbor generators. We make two observations that simplify the analysis below.

1. We drop $(\pm)$ in (54). This is justified as long as we analyze all near neighbor generators, or an appropriate subset that is invariant under multiplication by ± 1, (see (50), (51)).
2. For horizontal and helical interfaces the condition $\mathbf{r}_a = \mathbf{Q}^b_{\mathbf{x}(s_1) \cdot (\mathbf{f}_b - \mathbf{f}_a)}\mathbf{r}_b$ of Theorem 5.1 can be satisfied for all cases of (53). That is, we satisfy $\mathbf{r}_b = \hat{\mathbf{Q}}\mathbf{r}_a = \hat{\mathbf{Q}}\mathbf{r}$ by choosing $\mathbf{R_e}$ or $\mathbf{e}^\perp$ in (53) appropriately, i.e., choose $\hat{\mathbf{Q}} = \mathbf{Q}^b_{-(\mathbf{x}(s_1) \cdot (\mathbf{f}_b - \mathbf{f}_a))}$. We assume that this is done in all cases below where we discuss helical or horizontal interfaces. For these cases the condition (22) of orientability becomes

$$(\mathbf{y}_{a,p} \times \mathbf{y}_{a,q}) \cdot (\mathbf{y}_{b,p} \times \mathbf{y}_{b,q})(s) = \pm(\det\boldsymbol{\mu})(\mathbf{f} \cdot \mathbf{g}^\perp)^2 \big(\mathbf{r} \cdot \mathbf{Q}_{(\pm\boldsymbol{\mu}^T - \mathbf{I}) \cdot \mathbf{t})(s - s_1)}\mathbf{r}\big) > 0. \tag{55}$$

In Sections 7.2 and 7.3 below we treat separately the two cases in which the b phase generators are given by $\{\boldsymbol{\mu}^T\mathbf{f}, \boldsymbol{\mu}^T\mathbf{g}\}$ and $\{-\boldsymbol{\mu}^T\mathbf{f}, \boldsymbol{\mu}^T\mathbf{g}\}$. It will emerge below that these cases correspond to "slips" and "twins", respectively.

7.2. Examples: Slips

In this section, we choose $+$ of $\pm$ that occurs in Section 7.1. The group parameters are then $\{\mathbf{f}_a, \mathbf{g}_a\} = \{\mathbf{f}, \mathbf{g}\}$, which are required to satisfy the nondegeneracy conditions (27), and $\{\mathbf{f}_b, \mathbf{g}_b\} = \{\boldsymbol{\mu}^T\mathbf{f}, \boldsymbol{\mu}^T\mathbf{g}\}$. Thus, to obtain a locally compatible interface in the sense of Theorem 5.1, we need to find a $\boldsymbol{\mu} \in \mathcal{N}(GL(\mathbb{Z}^2))$ and $\mathbf{t} \in \mathbb{S}^1$ such that $(\mathbf{f}, \mathbf{g})^T(\boldsymbol{\mu} - \mathbf{I})\mathbf{t} = 0$. Since $(\mathbf{f}, \mathbf{g})^T$ is invertible by (27), the latter is equivalent to $(\boldsymbol{\mu} - \mathbf{I})\mathbf{t} = 0$. Notice that the existence of a slip is independent of the generators of the helical structure $\{\mathbf{f}, \mathbf{g}\}$. In other words, if a slip exists for one helical structure, then it is universal in the sense that an analogous slip exists for all the others. However, as in crystals, the loading (e.g., analogs of the Schmid stress) and atomic forces may favor some slips over others.

We first discuss orientable interfaces. Under the conditions assumed here, the formula (55) for orientability simplifies to $\det\boldsymbol{\mu} > 0$, and so we seek solutions for $\boldsymbol{\mu} \in \mathcal{N}^{(+)}(GL(\mathbb{Z}^2))$, excluding cases when there is no slip (i.e., $\boldsymbol{\mu} = \mathbf{I}$). We assume $0 \le (\mathbf{t} \cdot \mathbf{e}_2) \le 1$ without loss of generality. There are four cases in total:

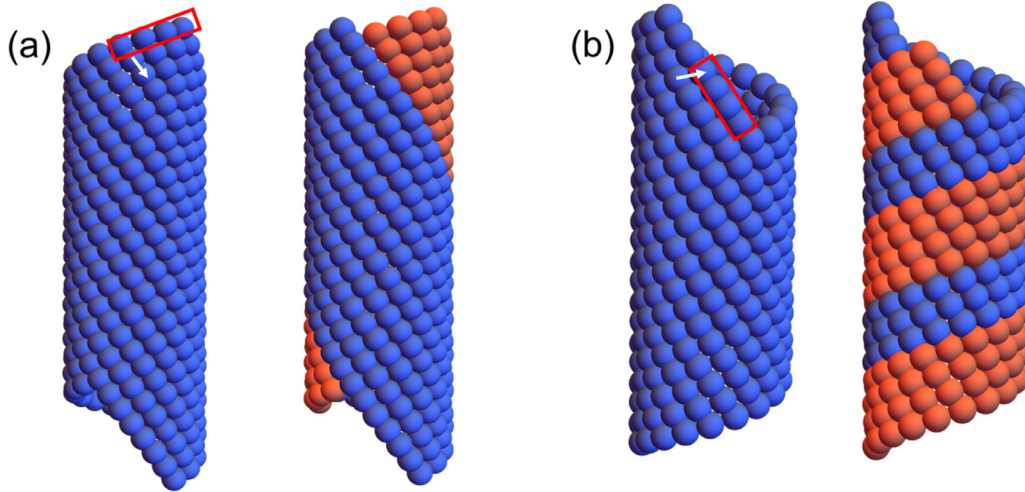(i) Slip along the nearest neighbor generator, i.e.,
- $\mathbf{t} = \begin{pmatrix} 1 \\ 0 \end{pmatrix}, \quad \boldsymbol{\mu} = \left\{ \begin{pmatrix} 1 & 1 \\ 0 & 1 \end{pmatrix}, \begin{pmatrix} 1 & -1 \\ 0 & 1 \end{pmatrix} \right\};$

(ii) Slip along the second nearest neighbor generator, i.e,
- $\mathbf{t} = \begin{pmatrix} 0 \\ 1 \end{pmatrix}, \quad \boldsymbol{\mu} = \left\{ \begin{pmatrix} 1 & 0 \\ 1 & 1 \end{pmatrix}, \begin{pmatrix} 1 & 0 \\ -1 & 1 \end{pmatrix} \right\}.$

The case (i) represent slip along closest-packed lines, i.e., lines of nearest neighbor atoms, and (ii) selects slip along next nearest neighbor atoms. Thus, the condition of orientability nicely selects the closest-packed directions among near

Fig. 4. Examples of slips. (a). Along the nearest neighbor generator: $\mathbf{t} = \mathbf{e}_1$, $\boldsymbol{\mu} = (\mathbf{e}_1, \mathbf{e}_1 + \mathbf{e}_2)$, $\mathbf{f} = (2\pi/35)(1, 2)$, $\mathbf{g} = 0.12(-2, 1)$. (b). Along the second nearest neighbor generator: $\mathbf{t} = \mathbf{e}_2$, $\boldsymbol{\mu} = (\mathbf{e}_1 + \mathbf{e}_2, \mathbf{e}_2)$, $\mathbf{f} = (2\pi/35)(1, 2)$, $\mathbf{g} = 0.12(-2, 1)$. The arrows indicate slip vectors (see (56)).
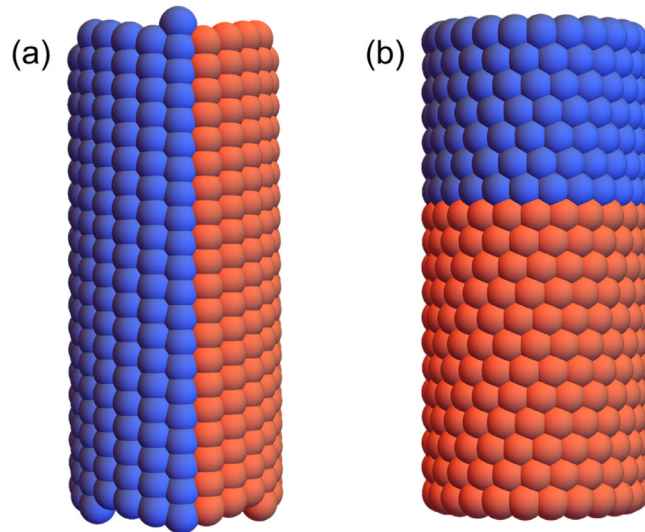
Fig. 5. Examples of vertical and horizontal twins. (a). A vertical twin with parameters $\mathbf{t} = \mathbf{e}_1$, $\boldsymbol{\mu} = (\mathbf{e}_1, \mathbf{e}_1 - \mathbf{e}_2)$, $\mathbf{f} = (\pi/12)\mathbf{e}_2$, $\mathbf{g} = 0.0625(4, 3)$. (b). A horizontal twin with parameters $\mathbf{t} = \mathbf{e}_1$, $\boldsymbol{\mu} = (-\mathbf{e}_1, -\mathbf{e}_1 + \mathbf{e}_2)$, $\mathbf{f} = (\pi/12)(1, .6)$, $\mathbf{g} = (\pi/12)\mathbf{e}_2$.

neighbor generators, which are expected to be favored by helical structures, as are the close-packed {111} family of planes in FCC crystals[8].

An elegant formula can be given for the tangent to the interface on the helical structure $\mathbf{t_y}$ that encodes all the parameters[9]:

$$\mathbf{t_y} = \frac{\nabla \mathbf{y}_a(\mathbf{0})\mathbf{t}}{|\nabla \mathbf{y}_a(\mathbf{0})\mathbf{t}|} = \frac{(\mathbf{f} \cdot \mathbf{t})\mathbf{Wr} + (\mathbf{g} \cdot \mathbf{t})\mathbf{e}}{\sqrt{|\mathbf{r}|^2(\mathbf{f} \cdot \mathbf{t})^2 + (\mathbf{g} \cdot \mathbf{t})^2}}. \tag{56}$$

The slip vectors corresponding to the examples in Fig. 4 are given by:

Slip Vector	Slip (a)	Slip (b)
$\mathbf{t_y}$	(0, 0.598974, -0.800769)	(0, 0.948429, 0.316989)

---

[8] The elementary reasoning in the two cases is the same: these are lines of atoms with least corrugation.

[9] We choose $\mathbf{x}(s_1) = \mathbf{0}$ in this formula without loss of generality.

Some non-orientable cases are also interesting, particularly for special loadings or special parameters. For example, in Fig. 4 a slip in the direction of any of the six atoms surrounding any atom might be considered reasonable, depending on atomic forces and loading. Also, we have six nearest neighbors. These *close packed helical structures* have non-orientable solutions of $(\boldsymbol{\mu} - \mathbf{I})\mathbf{t} = 0$, e.g., $\begin{pmatrix} 0 & -1 \\ -1 & 0 \end{pmatrix} \in \mathcal{N}^{(-)}(GL(\mathbb{Z}^2))$ with $\mathbf{t} = (1, -1)$.

7.3. Examples: Twins

In this section we choose - of $\pm$ that occurs in Section 7.1. The group parameters are then $\{\mathbf{f}_a, \mathbf{g}_a\} = \{\mathbf{f}, \mathbf{g}\}$ and $\{\mathbf{f}_b, \mathbf{g}_b\} = \{-\mathbf{f}, \mathbf{g}\}$, and they satisfy the non-degeneracy condition in (27). Thus, to obtain an *orientable locally compatible twin*, we require $\sigma = -\operatorname{sign}((\mathbf{f} \cdot \mathbf{g}^\perp)^2) = -1$, and we seek a $\boldsymbol{\mu} \in \mathcal{N}^{(-)}(GL(\mathbb{Z}^2))$ and $\mathbf{t} \in \mathbb{S}^1$ such that $((-\mathbf{f}, \mathbf{g})^T \boldsymbol{\mu} - (\mathbf{f}, \mathbf{g})^T)\mathbf{t} = 0$ and $(-\mathbf{f}, \mathbf{g})^T \boldsymbol{\mu} \neq (\mathbf{f}, \mathbf{g})^T$ (distinct phases). As indicated by the terminology, these solutions represent helical analogs of twinning. The solutions depend fundamentally on the given generators (i.e., akin to $\lambda_2 = 1$ for martensitic phase transformations (Chen et al., 2013; Gu et al., 2018)). This dependence can be catalogued based on the type of interface.

Lemma 7.1 (Twinning Lemma). *Let* $\{\mathbf{f}_{a,b}, \mathbf{g}_{a,b}\}$ *as above, subject to* (27) *and* $\sigma = -1$. *A helical structure with these parameters can form an orientable locally compatible twin, i.e.,* $((-\mathbf{f}, \mathbf{g})^T \boldsymbol{\mu} - (\mathbf{f}, \mathbf{g})^T)\mathbf{t} = 0$ *for* $\mathbf{t} \in \mathbb{S}^1$ *and* $\boldsymbol{\mu} \in \mathcal{N}^{(-)}(GL(\mathbb{Z}^2))$, *with* $(-\mathbf{f}, \mathbf{g})^T \boldsymbol{\mu} \neq (\mathbf{f}, \mathbf{g})^T$, *if and only if* $\boldsymbol{\mu}^T(-\mathbf{f}, \mathbf{g}) \neq (\mathbf{f}, \mathbf{g})$ *and*

  (i) *(Vertical Twin)* $\boldsymbol{\mu} \in \mathcal{N}^{(-)}(GL(\mathbb{Z}^2))$ *and* $\mathbf{t} \in \mathbb{S}^1$ *satisfy* $\boldsymbol{\mu}\mathbf{t} = \mathbf{t}$ *and* $\mathbf{t}^\perp \| \mathbf{f}$.
  (ii) *(Horizontal Twin)* $\boldsymbol{\mu} \in \mathcal{N}^{(-)}(GL(\mathbb{Z}^2))$ *and* $\mathbf{t} \in \mathbb{S}^1$ *satisfy* $\boldsymbol{\mu}\mathbf{t} = -\mathbf{t}$ *and* $\mathbf{t}^\perp \| \mathbf{g}$.
  (iii) *(Helical Twin)* $\boldsymbol{\mu} \in \mathcal{N}^{(-)}(GL(\mathbb{Z}^2))$ *and* $\mathbf{t} \in \mathbb{S}^1$ *are such that*

$$\mathbf{t} \text{ is not an eigenvector of } \boldsymbol{\mu}, \quad \mathbf{f} \| ((\boldsymbol{\mu} + \mathbf{I})\mathbf{t})^\perp, \quad \text{and} \quad \mathbf{g} \| ((\boldsymbol{\mu} - \mathbf{I})\mathbf{t})^\perp. \tag{57}$$

We postpone the proof to the end of this section and instead classify the solutions given by Lemma 7.1. We assume $0 \le (\mathbf{t} \cdot \mathbf{e}_2) \le 1$ without loss of generality. Where $\mathbf{f}$ or $\mathbf{g}$ are not assigned they are subject only to the hypotheses of Lemma 7.1. There are several cases:

(i) (Vertical Twins)
  • $\mathbf{t} = \begin{pmatrix} 1 \\ 0 \end{pmatrix}$, $\boldsymbol{\mu} \in \{ \begin{pmatrix} 1 & 1 \\ 0 & -1 \end{pmatrix}, \begin{pmatrix} 1 & -1 \\ 0 & -1 \end{pmatrix}, \begin{pmatrix} 1 & 0 \\ 0 & -1 \end{pmatrix} \}$, $\mathbf{f} \| \begin{pmatrix} 0 \\ 1 \end{pmatrix}$;
  • $\mathbf{t} = \begin{pmatrix} 0 \\ 1 \end{pmatrix}$, $\boldsymbol{\mu} \in \{ \begin{pmatrix} -1 & 0 \\ 1 & 1 \end{pmatrix}, \begin{pmatrix} -1 & 0 \\ -1 & 1 \end{pmatrix}, \begin{pmatrix} -1 & 0 \\ 0 & 1 \end{pmatrix} \}$, $\mathbf{f} \| \begin{pmatrix} 1 \\ 0 \end{pmatrix}$;
  • $\mathbf{t} = \frac{1}{\sqrt{2}} \begin{pmatrix} \pm 1 \\ 1 \end{pmatrix}$, $\boldsymbol{\mu} = \begin{pmatrix} 0 & \pm 1 \\ \pm 1 & 0 \end{pmatrix}$, $\mathbf{f} \| \begin{pmatrix} 1 \\ \mp 1 \end{pmatrix}$, respectively;
  • $\mathbf{t} = \frac{1}{\sqrt{5}} \begin{pmatrix} \pm 2 \\ 1 \end{pmatrix}$, $\boldsymbol{\mu} = \begin{pmatrix} 1 & 0 \\ \pm 1 & -1 \end{pmatrix}$, $\mathbf{f} \| \begin{pmatrix} \mp 1 \\ 2 \end{pmatrix}$, respectively;
  • $\mathbf{t} = \frac{1}{\sqrt{5}} \begin{pmatrix} \pm 1 \\ 2 \end{pmatrix}$, $\boldsymbol{\mu} = \begin{pmatrix} -1 & \pm 1 \\ 0 & 1 \end{pmatrix}$, $\mathbf{f} \| \begin{pmatrix} 2 \\ \mp 1 \end{pmatrix}$, respectively.
(ii) (Horizontal Twins) For each of the above, replace $\boldsymbol{\mu}$ by $-\boldsymbol{\mu}$ and switch $\mathbf{f}$ and $\mathbf{g}$.
(iii) (Helical Twins) Assume $m, n \in \mathbb{Z}$ with $n \ge 0$, $m^2 + n^2 \neq 0$.
  • $\mathbf{t} = \frac{1}{\sqrt{n^2+m^2}} \begin{pmatrix} m \\ n \end{pmatrix}$, $\boldsymbol{\mu} = \begin{pmatrix} 1 & 1 \\ 1 & 0 \end{pmatrix}$, $\mathbf{f} \| \begin{pmatrix} -m-n \\ 2m+n \end{pmatrix}$, $\mathbf{g} \| \begin{pmatrix} n-m \\ n \end{pmatrix}$;
  • $\mathbf{t} = \frac{1}{\sqrt{n^2+m^2}} \begin{pmatrix} m \\ n \end{pmatrix}$, $\boldsymbol{\mu} = \begin{pmatrix} 1 & -1 \\ -1 & 0 \end{pmatrix}$, $\mathbf{f} \| \begin{pmatrix} m-n \\ 2m-n \end{pmatrix}$, $\mathbf{g} \| \begin{pmatrix} m+n \\ -n \end{pmatrix}$;
  • $\mathbf{t} = \frac{1}{\sqrt{n^2+m^2}} \begin{pmatrix} m \\ n \end{pmatrix}$, $\boldsymbol{\mu} = \begin{pmatrix} 0 & 1 \\ 1 & 1 \end{pmatrix}$, $\mathbf{f} \| \begin{pmatrix} -m-2n \\ m+n \end{pmatrix}$, $\mathbf{g} \| \begin{pmatrix} -m \\ n-m \end{pmatrix}$;
  • $\mathbf{t} = \frac{1}{\sqrt{n^2+m^2}} \begin{pmatrix} m \\ n \end{pmatrix}$, $\boldsymbol{\mu} = \begin{pmatrix} 0 & -1 \\ -1 & 1 \end{pmatrix}$, $\mathbf{f} \| \begin{pmatrix} m-2n \\ m-n \end{pmatrix}$, $\mathbf{g} \| \begin{pmatrix} -m \\ n+m \end{pmatrix}$;
  • for each of the above, replace $\boldsymbol{\mu}$ by $-\boldsymbol{\mu}$ and switch $\mathbf{f}$ and $\mathbf{g}$.

The *twin vector* $\mathbf{t_y}$ on the helical structure is defined analogously to the slip vector in (56). The twin vectors for vertical and horizontal twins are $\mathbf{e}$ and $\mathbf{Wr}$, respectively, but the twin vectors for helical twins can take many forms. For instance, those corresponding to the examples in Fig. 6 are given by (in the $\{|\mathbf{r}|^{-1}\mathbf{r}, |\mathbf{r}|^{-1}\mathbf{Wr}, \mathbf{e}\}$ basis):

Twin Vector	Helical (a)	Helical (b)	Helical (c)	Helical (d)
$\mathbf{t_y}$	$\begin{pmatrix} 0 \\ -0.819123 \\ -0.573617 \end{pmatrix}$	$\begin{pmatrix} 0 \\ 0.785515 \\ 0.618842 \end{pmatrix}$	$\begin{pmatrix} 0 \\ 0.714072 \\ 0.700072 \end{pmatrix}$	$\begin{pmatrix} 0 \\ -0.68951 \\ 0.724277 \end{pmatrix}$

Proof of Lemma. 7.1. (i). Necessary and sufficient conditions are $\mathbf{g} \cdot (\boldsymbol{\mu}\mathbf{t} - \mathbf{t}) = 0$, $\mathbf{g} \cdot \mathbf{t} \neq 0$ and $\boldsymbol{\mu}\mathbf{t} \cdot \mathbf{f} = -\mathbf{f} \cdot \mathbf{t} = 0$ for some $\boldsymbol{\mu} \in \mathcal{N}^{(-)}(GL(\mathbb{Z}^2))$. The latter conditions imply $\mathbf{f} \| \mathbf{t}^\perp$ and $\boldsymbol{\mu}\mathbf{t} = \lambda\mathbf{t}$ for some $\lambda \in \mathbb{R}$. The two former conditions then imply $\lambda = 1$. This is necessary and sufficient so long as $\boldsymbol{\mu} \in \mathcal{N}^{(-)}(GL(\mathbb{Z}^2))$. (ii). This follows by the argument above after reversing the roles of $\mathbf{f}$ and $\mathbf{g}$ and replacing $\boldsymbol{\mu}$ with its minus. (iii). Necessary and sufficient conditions are $\mathbf{f} \cdot (\boldsymbol{\mu} + \mathbf{I})\mathbf{t} = 0$, $\mathbf{g} \cdot (\boldsymbol{\mu} - \mathbf{I})\mathbf{t} = 0$, $\mathbf{f} \cdot \mathbf{t} \neq 0$, $\mathbf{g} \cdot \mathbf{t} \neq 0$ and $\boldsymbol{\mu} \in \mathcal{N}^{(-)}(GL(\mathbb{Z}^2))$. There are linearly independent solutions $\{\mathbf{f}, \mathbf{g}\}$ of these two equations if and only
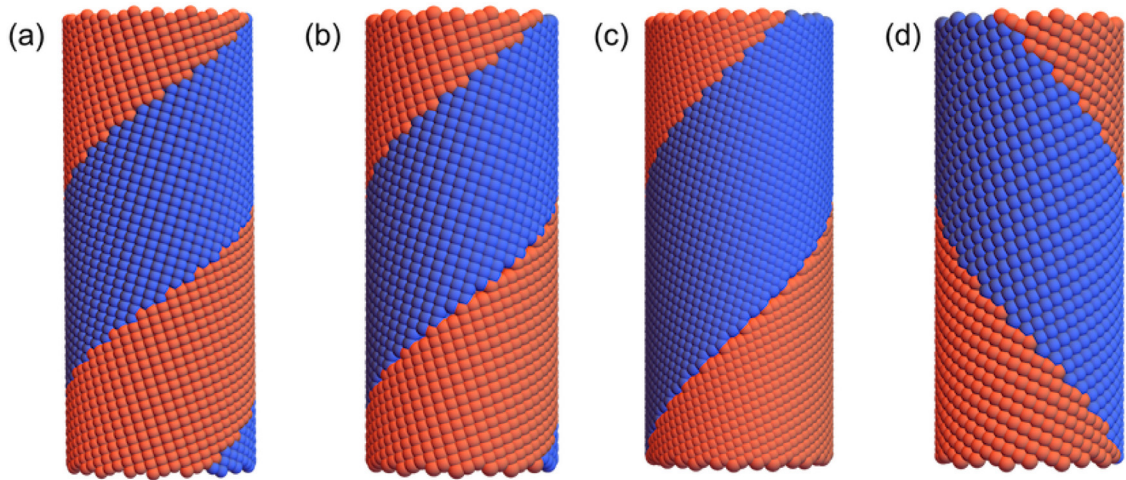
Fig. 6. Examples of helical twins. The parameter are: (a). $\mathbf{t} = (1/\sqrt{13})(3, -2)$, $\boldsymbol{\mu} = (\mathbf{e}_1 + \mathbf{e}_2, \mathbf{e}_1)$, $\mathbf{f} = (\pi/101)(-1, 4)$, $\mathbf{g} = -0.02(5, 2)$; (b). $\mathbf{t} = (1/\sqrt{13})(3, 2)$, $\boldsymbol{\mu} = (\mathbf{e}_1 - \mathbf{e}_2, -\mathbf{e}_1)$, $\mathbf{f} = (\pi/101)(1, 4)$, $\mathbf{g} = 0.0225(5, -2)$; (c). $\mathbf{t} = (1/\sqrt{13})(2, -3)$, $\boldsymbol{\mu} = (\mathbf{e}_2, \mathbf{e}_1 + \mathbf{e}_2)$, $\mathbf{f} = (\pi/154)(4, -1)$, $\mathbf{g} = -0.02(2, 5)$; (d). $\mathbf{t} = (1/\sqrt{13})(2, 3)$, $\boldsymbol{\mu} = (-\mathbf{e}_2, -\mathbf{e}_1 + \mathbf{e}_2)$, $\mathbf{f} = (\pi/101)(-4, -1)$, $\mathbf{g} = 0.03(-2, 5)$.

if $(\boldsymbol{\mu} + \mathbf{I})\mathbf{t}$ and $(\boldsymbol{\mu} - \mathbf{I})\mathbf{t}$ are not parallel. Note also that the conditions $\mathbf{f} \cdot \mathbf{t} \neq 0, \mathbf{g} \cdot \mathbf{t} \neq 0$ imply that $\boldsymbol{\mu}\mathbf{t} \neq \pm\mathbf{t}$. Hence, $(\boldsymbol{\mu} + \mathbf{I})\mathbf{t}$ and $(\boldsymbol{\mu} - \mathbf{I})\mathbf{t}$ are not parallel if and only if $\mathbf{t}$ is not an eigenvector of $\boldsymbol{\mu} \in \mathcal{N}^{(-)}(GL(\mathbb{Z}^2))$. $\square$

8. Discussion

We have developed a theoretical framework for investigating local compatibility between any two helical phases. This involves the description of the original helical group (Section 2), the nearest neighbor reparameterization of the group (Section 3), and the continuous compatibility conditions (Sections 4–6). Through rigorous justification, we have shown that there are four and only four types of locally compatible interface of a helical structure. These are vertical, horizontal, helical and elliptical interfaces—each named for their physical appearance on the structure. We have specialized these results to the case in which the two phases are the same and we have noticed that additional interfaces are possible when we allow near (as opposed to nearest) neighbor generators. We then classified the structural parameters under which near-neighbor-generated interfaces can form in a single phase; these are naturally interpreted as slips and twins (Section 7). In this section we discuss qualitatively some of the more striking features of helical structures that can be explored with this theoretical framework.

Mechanical twinning for large and reversible twist. If a helical structure has chirality or handedness, then twinning provides a promising mechanism to induce large macroscopic deformation at small elastic stress. Consider the example in Fig. 7. The blue phase atoms are arranged so that there is a line of atoms perfectly horizontal on the circumference of the cylinder and another line that loops around the cylinder in a "right-handed" fashion. When subject macroscopic twist, the
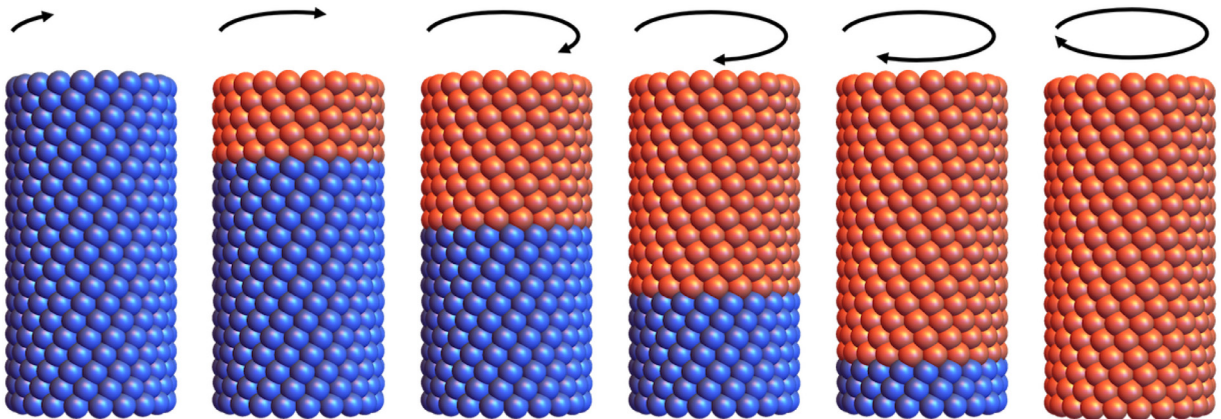
Fig. 7. Macroscopic twist induced by mechanical twinning at a horizontal interface. The parameters are $\mathbf{t} = \mathbf{e}_2$, $\boldsymbol{\mu} = (\mathbf{e}_1 - \mathbf{e}_2, -\mathbf{e}_2)$, $\mathbf{f} = (0.12, \pi/10)$, $\mathbf{g} = (-0.264, 0)$.
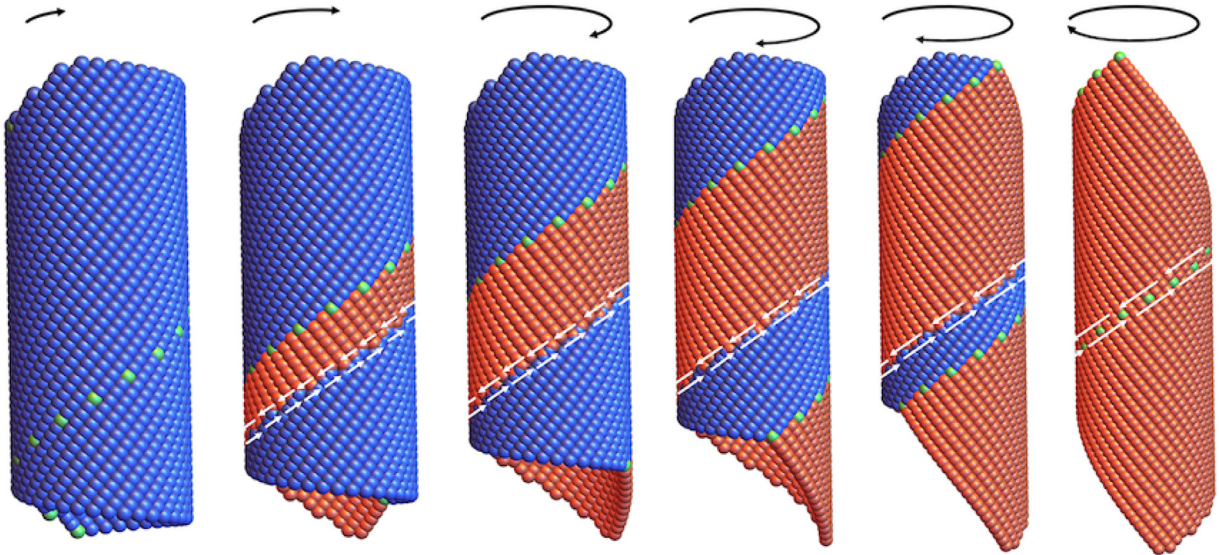
Fig. 8. Macroscopic twist and extension induced by twinning and slip at a helical interface. The parameters are $\mathbf{t} = (2, 3)$, $\boldsymbol{\mu} = (\mathbf{e}_1 + \mathbf{e}_2, \mathbf{e}_1)$, $\mathbf{f} = (\pi/88)(-5, 7)$ and $\mathbf{g} = 0.0225(1, 3)$. Points on the locally compatible interface are displayed in green. (For interpretation of the references to color in this figure legend, the reader is referred to the web version of this article.)

structure can accommodate the twist by deforming uniformly away from its preferred chirality at the cost of significant elastic stresses. But it has an alternative. Since its structural parameters satisfy the conditions of compatibility to form a horizontal twin, this structure can twist by the motion of twinned interfaces. Notice in the figure that the introduction of a twinned interface in this structure creates a mirrored (i.e., "left-handed") red phase, and the motion of this interface results in a change in volume fraction of the right and left handed phases. This corresponds to a macroscopic twist. More than that, if the initial phase is a stress-free equilibrium, then the mirrored phase and the mixtures should also be nearly stress-free (except, perhaps, close to the interface). So, we achieve large twisting deformation at little stress in a process that is (ideally) completely reversible.

Helical twins as the result of a phase transformation. The structural parameters that enable a horizontal twin are, unfortunately, quite restrictive. A horizontal line of atoms along the circumference is required, and this is far from generic[10]. On the other hand, many choices of parameters allow for locally compatible helical twins. It is tempting to think a similar correspondence between mechanical twinning and macroscopic deformation applies here, but helical interfaces are subject to a delicate notion of global compatibility. Consider the helical twin in Fig. 8.

Here, we resolve the local compatibility condition at the interface associated with the green atoms, so that neighboring atoms prior to transformation remain neighbors across this interface after transformation. However, helical interfaces come in pairs—the blue phase is above the red phase for the locally compatible interface, but there is a second interface with the opposite orientation. The correspondence of atoms across this second interface may look perfect, but any motion involving a change in the volume fraction of the phases, such as the one shown in the figure, *necessarily results in slip*. Thus, mechanical twist in these instances is achieved only through a combination of twinning and slip. Consequently, the volume fraction of phases for these interfaces is, in a certain sense, topologically protected.

This leads to a fundamental question: Can any of the helical interfaces be achieved without slip? The answer is yes, and potentially generically so (though, there is still much to discover in this direction). The setting is that of a phase transformation as shown in Fig. 9. A helical structure, initially of a certain preferred chirality (green), is subject to a stimuli which changes its free energy so that a second chirality (blue and its mirror in red) becomes the preferred state. The two phases may satisfy the conditions of local compatibility along a helical interface, but they will be unable to coexist as pairs without slip due to the global compatibility condition discussed above. However, by twinning the second phase at exactly the right volume fraction—so that it accommodates the chirality of the first phase—we can achieve a globally compatible helical structure that involves no slip and no elastic stresses, all while cycling back and forth between phases. This is a fascinating analog of ideas of self-accommodation and $\lambda_2 = 1$ for crystalline solids undergoing phase transformations (Bhattacharya, 1992; Chen et al., 2013; Gu et al., 2018).

Vertical interfaces in microtubules. As a final comment to emphasize the importance of compatible interfaces in helical structures, we introduce a biological example: the fission yeast end binding protein (EB1) homolog Mal3p in microtubules (Sandblad et al., 2006). Microtubules are dynamic tubular structures involved in intracellular transport, flagellar motion,

---

[10] Although it may be induced by a particular macroscopic twist and extension in a structure that does not exhibit this feature in the stress-free state.
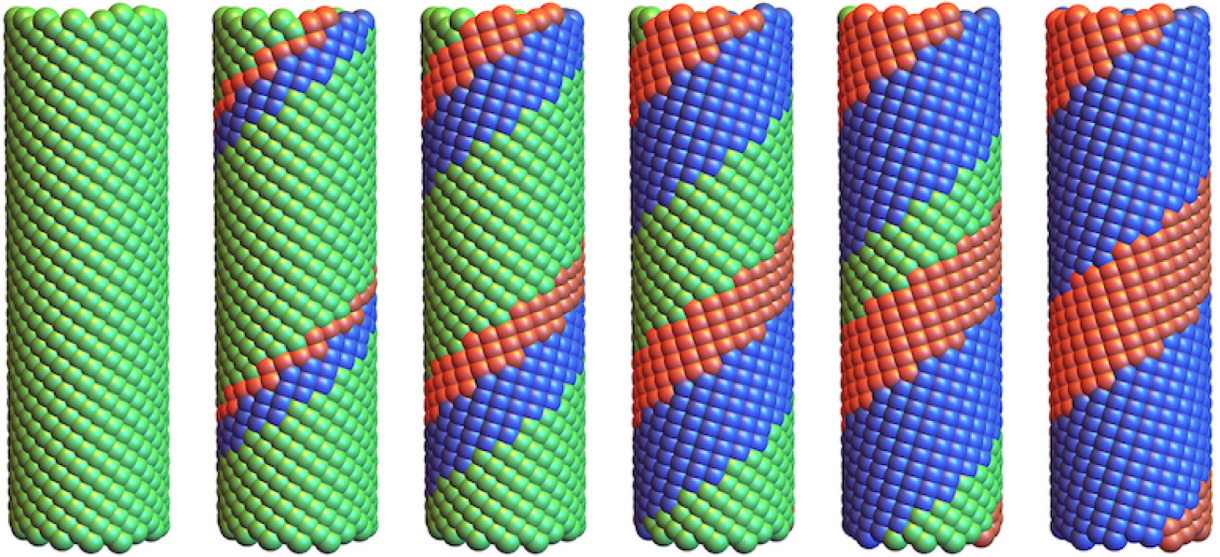
Fig. 9. A phase transition results in a helical interface. The reference tangent $\mathbf{t} = (3, -2)$. The helical twin has parameters $\mathbf{f} = (\pi/55)(-1, 4)$, $\mathbf{g} = 0.04(-5, -2)$ and $\boldsymbol{\mu} = (\mathbf{e}_1 + \mathbf{e}_2, \mathbf{e}_1)$. The parent phase has parameters $(\bar{\mathbf{f}}, \bar{\mathbf{g}}) = \lambda(\mathbf{f}, \mathbf{g}) + (1 - \lambda)(-\boldsymbol{\mu}^T \mathbf{f}, \boldsymbol{\mu}^T \mathbf{g})$ for $\lambda = 0.6$.
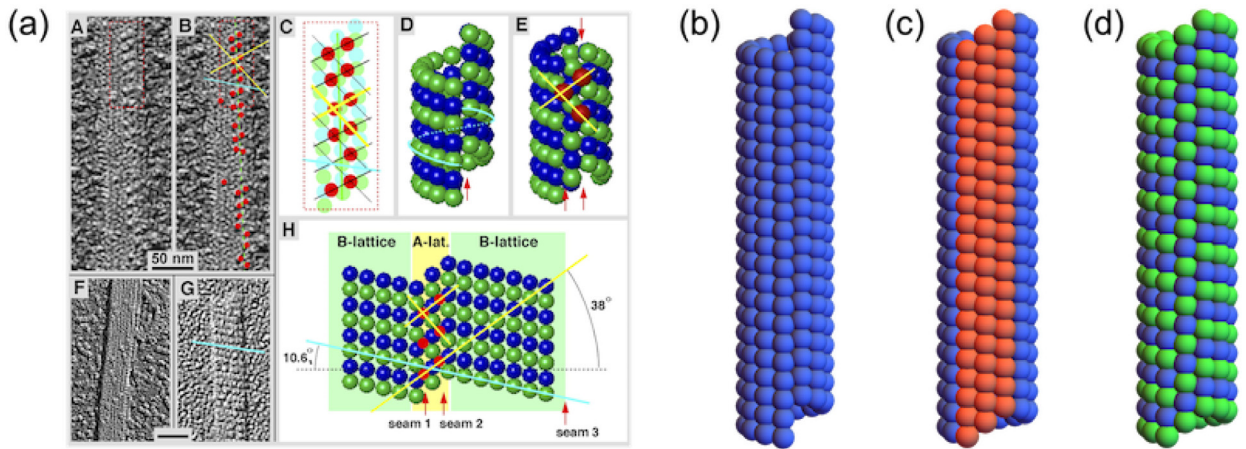
Fig. 10. Vertical interfaces in a microtubule. (a). The microtubule lattice seam and compatible vertical interfaces (Reproduced with permission (Sandblad et al., 2006) ©2006 Elsevier Inc.). (b–d) A 13 protofilaments microtubule constructed by our method. (b) The lattice seam created by wrapping the "B" lattice to form a tube. (c,d) The microtubule as the combination of "A" and "B" phases. These form compatible vertical interfaces. The parameters are: (Blue) $\mathbf{f}_a = (2\pi/13, 0)$, $\mathbf{g}_a = (\frac{2\pi}{13} \tan(\frac{-10.6\pi}{180}), 2\pi/13)$. (Red) $\mathbf{f}_b = (2\pi/13, 0)$, $\mathbf{g}_b = (\frac{2\pi}{13} \tan(\frac{38\pi}{180}), 2\pi/13)$ and $\boldsymbol{\mu} = \mathbf{I}$. The reference tangent is $\mathbf{t} = (0, 1)$.

and many other tasks in cells. Their structure is often that of a non-discrete helical group. Specifically, in the example shown in Fig. 10(a), the preferred "B" lattice is described by the angle 10.6° when unrolled. However, wrapping this "B" lattice onto a tubular structure leads to a large vertical seam on the tube 10(b). *This is non-discreteness.* The authors in Sandblad et al. (2006) argue that this seam, in particular, is much too large for the microtubule to be stable in this structure. Instead, the microtubule forms a vertical strip corresponding to the "A" lattice depicted in 10(a). This has the effect of stabilizing the structure by making the seam more coherent. In the context of our theoretical framework, this mechanism is exactly that of compatible vertical interfaces between the two phases (Fig. 10(c,d)).

Besides the microtubule, there are many possible applications of these results to nanotubes, inorganic or biological, and also larger scale structures like helical origami (Feng et al., 2019). In this paper we have concentrated on the basic theory, especially the classification of *all possible* compatible interfaces and their mobility. In forthcoming work, we will apply this theory to interesting special cases, especially to guide the design of structure-dependent tension-twist protocols that can induce specific phase transformations.

Acknowledgment

Appendix A. Reparameterization of the helical groups - the proofs

Proof of the nearest neighbor reparameterization algorithm. Let G and $\mathbf{y}(n, m)$ be as defined in Section 3. A nearest neighbor reparameterization implies that nearest (and next to nearest) neighbors of the reparameterized structure correspond to nearest neighbors of $(0,0)$ in the 2D lattice $\mathbb{Z}^2$. Thus, we consider

$$dist^2(n, m) = |\mathbf{y}(n, m) - \mathbf{y}(0, 0)|^2 = |(\mathbf{Q}_{m\theta+n\alpha} - \mathbf{I})(\mathbf{p} - \mathbf{z}) + m\tau\mathbf{e}|^2 = 4r^2 \sin^2\left(\frac{m\theta + n\alpha}{2}\right) + m^2\tau^2, \tag{58}$$

where $r = |\mathbf{p} - \mathbf{z}|$ (and subject to appropriate constraints).

Nearest and second nearest neighbors are obtained by minimizing[11] $dist^2(n, m)$ over integers m, n with $n \in \{-i, \ldots, 0, \ldots, i\}$. Let m_0 be the smallest integer greater than $2r^2/\tau^2 - 1/2$. No minimizer of (58) can have $|m| > m_0$, because, otherwise, decreasing $|m|$ by one decreases $dist^2$. Thus, since $n \in \{-i, \ldots, 0, \ldots, i\}$, the minimization of $dist^2(n, m)$ is a finite integer minimization problem, and both first and second nearest neighbors can always be found. However, we have non-uniqueness because $dist^2(n, m) = dist^2(-n, -m)$, and there may be additional degeneracy.

Since we have the existence of minimizers, we can suppose a minimizer of $dist^2(m, n)$ is given by (n_1, m_1), $n_1 \in \{-i, \ldots, 0, \ldots, i\}$. Further, we can consider the auxiliary minimization problem

$$\min_{m,n}\{dist^2(n, m) : m_1 n \neq n_1 m\}, \tag{59}$$

and suppose (n_2, m_2), $n_2 \in \{-i, \ldots, 0, \ldots, i\}$ is a minimizer to this problem. Hence, we study the group elements $g_1 = g(n_1, m_1)$ and $g_2 = g(n_2, m_2)$. Here, we call g_1 the *nearest neighbor generator* and g_2 is the *second nearest neighbor generator*[12]. The meaning of the constraint $m_1 n_2 \neq m_2 n_1$ is explained in detail below, but clearly it serves to rule out $n_2 = -n_1, m_2 = -m_1$ and other behavior such as $g_1^2 = g_2$ which would be problematic for a concept of compatibility.

We will show that the given group G is generated by the nearest neighbor generators g_1 and g_2. Let

$$G' = \{g_1^p g_2^q : (p, q) \in \mathbb{Z}^2\}, \quad \text{(omit repeated elements)}. \tag{60}$$

Since g_1 and g_2 are both elements of the group G (as well as their products), G' is a subgroup of G. To show that $G' = G$, we will argue by contradiction. The basic idea is to define a unit cell[13] based on g_1 and g_2. Since these are nearest neighbor generators, this unit cell contains a single atom at one of the vertices. However, in supposing that $G' \neq G$, we will argue that there must be another atom inside this unit cell. This is the desired contradiction.

To define the unit cell, we first note that the formula $g_1^p g_2^q$ also makes sense when p and q are real numbers. The two vectors

$$\frac{d}{d\xi} g_1^\xi(\mathbf{p})|_{\xi=0}, \quad \frac{d}{d\eta} g_2^\eta(\mathbf{p})|_{\eta=0}, \tag{61}$$

define tangent vectors on the cylindrical surface $\mathcal{C} = \{\mathbf{z} + r(\cos\omega\,\mathbf{e}_1 + \sin\omega\,\mathbf{e}_2) + \zeta\mathbf{e} : 0 < \omega \leq 2\pi, \ \zeta \in \mathbb{R}\}$ where $\mathbf{e}_1, \mathbf{e}_2, \mathbf{e}$ are orthonormal. These two tangents are not parallel since by construction $m_1 n_2 \neq m_2 n_1$. We call this condition the *non-degeneracy condition*[14]. Hence,

$$\mathcal{U} = \{(g_1^\xi(\mathbf{p}), g_2^\eta(\mathbf{p})) : 0 \leq \xi < 1, \ 0 \leq \eta < 1\} \subset \mathcal{C} \tag{62}$$

is a unit cell for G' and has positive area.

To show $G' = G$, we argue by contradiction. We suppose that there are integers $\tilde{n}, \tilde{m}$ such that the isometry $\tilde{g} = g(\tilde{n}, \tilde{m}) \in G$ but $\tilde{g} \notin G'$. Let $\xi, \eta \in \mathbb{R}$ satisfy

$$\tilde{m} = \xi m_1 + \eta m_2 \quad \tilde{n} = \xi n_1 + \eta n_2. \tag{63}$$

Note that (63) is solvable for $(\xi, \eta) \in \mathbb{R}^2$ because we have assumed $m_1 n_2 \neq n_1 m_2$. Since $\tilde{g} \notin G'$, $(\tilde{m}, \tilde{n})$ are not both zero and at least one of ξ and η is not an integer. By subtracting suitable integers from $\tilde{m}$ and $\tilde{n}$, we can assume without loss of generality that $\xi, \eta \in [-1/2, 1/2]$ and ξ, η are not both zero.

---

[11] In this formula, we have chosen the reference atom $\mathbf{y}(0, 0)$ simply for convenience. Notice that the distance from the reference atom to its nearest and next nearest neighbors is independent of the particular choice of reference atom. For this reason, we are free to make this choice.

[12] It is possible for $dist(n_1, m_1) = dist(n_2, m_2)$, in which case the second nearest neighbor is actually the also the nearest neighbor.

[13] A *unit cell* in this case is the direct analog of that for the translation group, i.e., the images of the unit cell under the group cover the cylinder $\mathcal{C}$ defined just after (61), and images corresponding to distinct group elements are distinct.

[14] If $m_1 n_2 = m_2 n_1$, then the two functions $g_1^\xi(\mathbf{p}), g_2^\eta(\mathbf{p})$ parameterize the same curve on the cylinder. In this case, g_1 and g_2 cannot be used to define a unit cell of the cylinder.

We make the standing assumption on θ and α that $-\pi/2 \leq m_1\theta + n_1\alpha \leq \pi/2$ and $-\pi/2 \leq m_2\theta + n_2\alpha \leq \pi/2$. These reasonable assumptions imply that the unit cell $\mathcal{U}$ does not extend more than halfway around the cylinder $\mathcal{C}$. We also note that $\sin^2(\delta/2)$ is a strictly convex, even function of δ on the interval $-\pi/2 \leq \delta \leq \pi/2$. Then, using the distance formula in (58), we have that

$$|g_1^\xi g_2^\eta(\mathbf{p}) - \mathbf{p}|^2 = 4r^2\sin^2\left(\frac{\xi(m_1\theta+n_1\alpha)+\eta(m_2\theta+n_2\alpha)}{2}\right) + (\xi m_1 + \eta m_2)^2\tau^2. \tag{64}$$

By changing g_1 or g_2 to its inverse, if necessary (which does not change the distances $|g_{1,2}(\mathbf{p}) - \mathbf{p}|$), we can assume that $m_1 \geq 0$, $m_2 \geq 0$.

Using the evenness of $\sin^2$ (i.e., $\sin^2(\delta/2) = \sin^2(|\delta|/2)$) and its monotonicity on the interval $(0, \pi/2)$, we observe that

$$\sin^2\left(\frac{\xi(m_1\theta+n_1\alpha)+\eta(m_2\theta+n_2\alpha)}{2}\right) = \sin^2\left(\frac{|\xi(m_1\theta+n_1\alpha)+\eta(m_2\theta+n_2\alpha)|}{2}\right)$$

$$\leq \sin^2\left(\frac{(1/2)|(m_1\theta+n_1\alpha)|+(1/2)|(m_2\theta+n_2\alpha)|}{2}\right)$$

$$\leq \frac{1}{2}\sin^2\left(\frac{m_1\theta+n_1\alpha}{2}\right) + \frac{1}{2}\sin^2\left(\frac{m_2\theta+n_2\alpha}{2}\right). \tag{65}$$

since $\xi, \eta \in [-1/2, 1/2]$. Here, the last step follows from the convexity of $\sin^2(\delta/2)$ on $[-\pi/2, \pi/2]$. This calculation, together with the observation $(\xi m_1 + \eta m_2)^2 \leq (1/4)(m_1+m_2)^2$, shows that

$$|g_1^\xi g_2^\eta(\mathbf{p}) - \mathbf{p}|^2 \leq \frac{1}{2}|g_1(\mathbf{p}) - \mathbf{p}|^2 - (\tau^2/2)m_1^2 + \frac{1}{2}|g_2(\mathbf{p}) - \mathbf{p}|^2 - (\tau^2/2)m_2^2 + (\tau^2/4)(m_1+m_2)^2$$

$$\leq |g_2(\mathbf{p}) - \mathbf{p}|^2 - (\tau^2/4)(m_2-m_1)^2 \leq |g_2(\mathbf{p}) - \mathbf{p}|^2. \tag{66}$$

Here we have used that $g_2(\mathbf{p})$ is a *second* nearest neighbor of $\mathbf{p} \in \mathcal{C}$. Following back through the inequalities, we see that equality holds in (66) only if $g_1 = g_2$ which is forbidden by our hypothesis $m_1 n_2 \neq m_2 n_1$. And also $g_1^\xi g_2^\eta \neq g_1$ by this hypothesis. Thus we reach the conclusion that $|g_1^\xi g_2^\eta(\mathbf{p}) - \mathbf{p}| < |g_2(\mathbf{p}) - \mathbf{p}|$ which contradicts that $g_2(\mathbf{p})$ is a second nearest neighbor of $\mathbf{p}$. Hence, $G' = G$.

Proof of the algorithm for the domain of powers of the nearest neighbor generators. Let the nearest neighbor generators $g_1 = g(n_1, m_1)$ and $g_2 = g(n_2, m_2)$ be given as in the first algorithm in Section 3 so that $m_1 n_2 \neq m_2 n_1$ with $n_1, n_2 \in \{-i, \ldots, 0, \ldots, i\}$. Recall also from Section 3 that there are infinitely many $(p, q) \in \mathbb{Z}^2$ such the $g_1^p g_2^q = id$, and these solve (14) for the appropriate choice of $n \in \mathbb{Z}$. Note that, in this equation, the integers m_1 and m_2 cannot both be zero. So we first assume $m_1 \neq 0$.

From these solutions and the assumption $m_1 \neq 0$, there is a unique solution $(p^\star, q^\star) \in \mathbb{Z}^2$ of $(p, q) \neq (0, 0)$ with $g_1^p g_2^q = id$ that contains the smallest positive value of q. We claim that $\mathcal{D} = \mathbb{Z} \times \{1, \ldots, q^\star\}$ serves as a domain for the powers (p, q) with the property that there are no repeated elements.

To see this, note first that any $q \in \mathbb{Z}$ is expressible in the form $q = jq^\star + q'$ where $j \in \mathbb{Z}$ and $q' \in \{1, \ldots, q^\star\}$. Thus, $g_1^p g_2^q = g_1^{p'+jp^\star} g_2^{q'+jq^\star} = g_1^{p'} g_2^{q'}$, so the powers (p, q) of any group element can be assumed to lie in $\mathcal{D}$.

Thus we only need to show that two distinct pairs of powers $(p, q) \in \mathcal{D}$ and $(p', q') \in \mathcal{D}$ do not give the same group element. To see this, assume that $g_1^p g_2^q = g_1^{p'} g_2^{q'}$ for $q, q' \in \{1, \ldots, q^\star\}$ and, without loss of generality, $q \geq q'$. Then

$$g_1^{p-p'} g_2^{q-q'} = id. \tag{67}$$

By the minimality property of $q^\star$, this implies that $q = q'$, and (67) is reduced to $g_1^{p-p'} = id$. The latter is possible under the condition $m_1 \neq 0$ and the assumptions on the group parameters τ, $\mathbf{z}$ if and only if $p = p'$. We have shown that each point $(p, q) \in \mathcal{D}$ (using nearest-neighbor generators g_1, g_2) corresponds to one and only one element of G.

In this argument, we made the additional hypothesis that $m_1 \neq 0$. This is without loss of generality. Note that the condition $n_1 m_2 - n_2 m_1 \neq 0$ forbids m_1 and m_2 to vanish simultaneously. Thus if $m_1 = 0$, then $m_2 \neq 0$. Consequently, we can simply replace g_1 with g_2 and g_2 with g_1 if this is the case. This generates the same structure.

So far, we have deduced that $G = \{g_1^p g_2^q : (p, q) \in \mathcal{D}\}$ (with $m_1 \neq 0$), and this description has no repeated elements. It follows from a slight modification of the proof given above that an alternative description of this group is $G = \{g_1^p g_2^q : (p, q) \in \mathcal{D}_{q_0}\}$ where $\mathcal{D}_{q_0} = (0, q_0) + \mathcal{D} = \mathbb{Z} \times \{q_0 + 1, \ldots, q_0 + q^\star\}$ for any integer q_0.

Supplementary material

Supplementary material associated with this article can be found, in the online version, at doi:10.1016/j.jmps.2019.06.014.

References

Arisaka, F., Engel, J., Klump, H., 1981. Contraction and dissociation of the bacteriophage T4 tail sheath induced by heat and urea. Prog. Clin. Biol. Res. 64, 365–379.

Asakura, S., 1970. Polymerization of flagellin and polymorphism of flagella. Adv. Biophys. 1, 99.

Ball, J.M., James, R.D., 1987. Fine phase mixtures as minimizers of energy. Arch. Ration. Mech. Anal. 100 (1), 13–52. doi:10.1007/BF00281246.

Ball, J.M., James, R.D., 1992. Proposed experimental tests of a theory of fine microstructure and the two-well problem. Philos. Trans. R. Soc. Lond. A Math. Phys. Eng. Sci. 338 (1650), 389–450. doi:10.1098/rsta.1992.0013.

Banerjee, A.S., 2013. Density functional methods for objective structures: theory and simulation schemes. Ph.D. thesis; University of Minnesota, Minneapolis.

Banerjee, A.S., Elliott, R.S., James, R.D., 2015. A spectral scheme for Kohn–Sham density functional theory of clusters. J. Comput. Phys. 287, 226–253. doi:10.1016/j.jcp.2015.02.009.

Banerjee, A.S., Suryanarayana, P., 2016. Cyclic density functional theory: a route to the first principles simulation of bending in nanostructures. J. Mech. Phys. Solids 96, 605–631.

Bhattacharya, K., 1992. Self-accommodation in martensite. Arch. Ration. Mech. Anal. 120 (3), 201–244. doi:10.1007/BF00375026.

Calladine, C.R., 1975. Construction of bacterial flagella. Nature 255 (5504), 121.

Chen, X., Srivastava, V., Dabade, V., James, R.D., 2013. Study of the cofactor conditions: conditions of supercompatibility between phases. J. Mech. Phys. Solids 61 (12), 2566–2587. doi:10.1016/j.jmps.2013.08.004.

Chluba, C., Ge, W., de Miranda, R.L., Strobel, J., Kienle, L., Quandt, E., Wuttig, M., 2015. Ultralow-fatigue shape memory alloy films. Science 348 (6238), 1004–1007.

Cui, J., Chu, Y.S., Famodu, O.O., Furuya, Y., Hattrick-Simpers, J., James, R.D., Ludwig, A., Thienhaus, S., Wuttig, M., Zhang, Z., et al., 2006. Combinatorial search of thermoelastic shape-memory alloys with extremely small hysteresis width. Nat. Mater. 5 (4), 286.

Dayal, K., Elliott, R., James, R. D., 2018. Objective formulas. In preparation.

Dumitrică, T., James, R.D., 2007. Objective molecular dynamics. J. Mech. Phys. Solids 55 (10), 2206–2236. doi:10.1016/j.jmps.2007.03.001.

Falk, W., James, R.D., 2006. Elasticity theory for self-assembled protein lattices with application to the martensitic phase transition in bacteriophage T4 tail sheath. Phys. Rev. E 73 (1), 011917.

Feng, F., Plucinsky, P., James, R. D., 2019. Helical miura origami. arXiv:1902.05123.

Ganor, Y., Dumitrică, T., Feng, F., James, R.D., 2016. Zig–zag twins and helical phase transformations. Philos. Trans. R. Soc. A 374 (2066), 20150208.

Ghose, S., Banerjee, A.S., Suryanarayana, P., 2019. Symmetry-adapted real-space density functional theory for cylindrical geometries: application to large X (X = C, Si, Ge, Sn) nanotubes. arXiv preprint arXiv:1904.13356.

Goldberger, J., He, R., Zhang, Y., Lee, S., Yan, H., Choi, H.-J., Yang, P., 2003. Single-crystal gallium nitride nanotubes. Nature 422 (6932), 599.

Gu, H., Bumke, L., Chluba, C., Quandt, E., James, R.D., 2018. Phase engineering and supercompatibility of shape memory alloys. Mater. Today 21, 265–277. doi:10.1016/j.mattod.2017.10.002.

He, Y.-J., Sun, Q.-P., 2009. Scaling relationship on macroscopic helical domains in NiTi tubes. Int. J. Solids Struct. 46 (24), 4242–4251.

James, R.D., 2006. Objective structures. J. Mechanics and Physics of Solids 54 (11), 2354–2390. doi:10.1016/j.jmps.2006.05.008.

James, R.D., 2015. Taming the temperamental metal transformation. Science 348 (6238), 968–969. doi:10.1126/science.aab3273.

James, R.D., Hane, K.F., 2000. Martensitic transformations and shape-memory materials. Acta Mater. 48 (1), 197–222. doi:10.1016/S1359-6454(99)00295-5.

James, R.D., Zhang, Z., 2005. A way to search for multiferroic materials with unlikely combinations of physical properties. In: Planes, A., Manõsa, L., Saxena, A. (Eds.), Magnetism and Structure in Functional Materials, Springer Series in Materials Science, 9. Springer-Verlag, Berlin, pp. 159–175.

Komai, R.K., 2015. Chirality switching by martensitic transformation in protein cylindrical crystals: application to bacterial flagella. Ph.D. Thesis. Northwestern University, Chicago.

Moody, M.F., 1967. Structure of the sheath of bacteriophage T4: I. structure of the contracted sheath and polysheath. J. Mol. Biol. 25 (2), 167–200.

Moody, M.F., 1973. Sheath of bacteriophage T4: III. Contraction mechanism deduced from partially contracted sheaths. J. Mol. Biol. 80 (4), 613–635.

Ni, X., Greer, J.R., Bhattacharya, K., James, R.D., Chen, X., 2016. Exceptional resilience of small-scale au$_{30}$cu$_{25}$zn$_{45}$ under cyclic stress-induced phase transformation. Nano Lett. 16 (12), 7621–7625.

Olson, G.B., Hartman, H., 1982. Martensite and life: displacive transformations as biological processes. Le J. de Phys. Colloq. 43 (C4), C4–855.

Pitteri, M., Zanzotto, G., 2002. Continuum Models for Phase Transitions and Twinning in Crystals. CRC Press.

Radisavljevic, B., Radenovic, A., Brivio, J., Giacometti, I.V., Kis, A., 2011. Single-layer MoS$_2$ transistors. Nat. Nanotechnol. 6 (3), 147.

Sandblad, L., Busch, K.E., Tittmann, P., Gross, H., Brunner, D., Hoenger, A., 2006. The schizosaccharomyces pombe eb1 homolog mal3p binds and stabilizes the microtubule lattice seam. Cell 127 (7), 1415–1424. doi:10.1016/j.cell.2006.11.025.

Song, Y., Chen, X., Dabade, V., Shield, T.W., James, R.D., 2013. Enhanced reversibility and unusual microstructure of a phase-transforming material. Nature 502 (7469), 85–88.

Yonekura, K., Maki-Yonekura, S., Namba, K., 2003. Complete atomic model of the bacterial flagellar filament by electron cryomicroscopy. Nature 424 (6949), 643.

Zarnetta, R., Takahashi, R., Young, M.L., Savan, A., Furuya, Y., Thienhaus, S., Maaß, B., Rahim, M., Frenzel, J., Brunken, H., et al., 2010. Identification of quaternary shape memory alloys with near-zero thermal hysteresis and unprecedented functional stability. Adv. Funct. Mater. 20 (12), 1917–1923.

Zhang, D.-B., Dumitrică, T., Seifert, G., 2010. Helical nanotube structures of MoS$_2$ with intrinsic twisting: an objective molecular dynamics study. Phys. Rev. Lett. 104 (6), 065502.

Zhang, Z., James, R.D., Müller, S., 2009. Energy barriers and hysteresis in martensitic phase transformations. Acta Mater. 57 (15), 4332–4352.

Zhou, J., Li, N., Gao, F., Zhao, Y., Hou, L., Xu, Z., 2014. Vertically-aligned BCN nanotube arrays with superior performance in electrochemical capacitors. Sci. Rep. 4, 6083.